Environment, Development and Sustainability (2024) 26:33–88
https://doi.org/10.1007/s10668-022-02737-1

REVIEW

A comprehensive review on the recent development of inorganic nano-adsorbents for the removal of heavy metals from water and wastewater

Danial Nayeri[1,2] · Seyyed Alireza Mousavi[1]

Received: 14 October 2021 / Accepted: 22 October 2022 / Published online: 30 November 2022

Abstract
Nowadays, the removal of heavy metals (HMs) as one of the major environmental pollutants has become an obvious issue in preserving the environment. Among the suggested approaches, the use of nano-adsorbents has been immensely contributed for the treatment of contaminated water and wastewater by HMs because of their unique physicochemical characteristics. Herein, we are offering a potent view on adsorption mechanism of different inorganic nano-adsorbent classes with special focus on the main characteristics (BET, SEM/FESEM, FTIR, and XRD), reviewing the effects of several operational factors (initial concentration of HMs, adsorbent dosage, contact time, and pH) on the HMs removal. Furthermore, the importance of isotherm-kinetic models has been discussed. Eventually, the negative effects of nanoparticles in environment are exclusively reviewed. This comprehensive review demonstrated that inorganic nano-adsorbents have a crystalline structure with a different diameter size range of 10–80 nm, which can be a promising candidate (high efficiency $^{>}$90%) and large surface area for HMs decontamination. The results of the comparison between the isotherm-kinetic models also confirmed that the experimental data were fitted with Langmuir isotherm ($R^{2\,>}$0.98) and PSO kinetics ($R^{2\,>}$0.98), respectively.

Keywords Nano-adsorbents · Heavy metals · Carbon nanotubes · Magnetic nanoparticles · Isotherm and kinetics

1 Introduction

In recent decades, water pollution as a global challenge has been gained numerous attention among the environmentalists due to its negative effects on the natural ecosystem and human health (Sharifpour et al., 2018). The increasing rate of urbanization, industrialization, and globalization has caused severe environmental concerns such as

✉ Seyyed Alireza Mousavi
seyyedarm@yahoo.com; sar.mousavi@kums.ac.ir

[1] Department of Environmental Health Engineering, School of Public Health, Kermanshah University of Medical Sciences, Kermanshah, Iran

[2] Student Research Committee, Kermanshah University of Medical Sciences, Kermanshah, Iran

water quality deterioration. Access to sufficient water with good quality is also recognized as an important development index by all governments around the world (Emmanuel Alepu Odey & Harrison Ikhumhen, 2017; Kumar et al., 2017; Patil et al., 2019). Among the pollutants, heavy metals (HMs) such as zinc (Zn), arsenic (As), copper (Cu), cadmium (Cd), chromium (Cr), mercury (Hg), nickel (Ni), and lead (Pb) can inflict considerable harm to animals and humans even at basic levels (Bora & Dutta, 2019; Madala et al., 2017; Razmgar & Mokhtari Hosseini, 2016; Shan et al., 2020; Sirviö & Visanko, 2020). Because of their special properties such as acute toxicity, accumulation potential, solubility in aqueous media, and capability to bind with proteins, enzymes and nucleic acids, heavy metals are categorized as a class of persistent toxic substances (PTSs) (Akbarzadeh et al., 2020; Zhang et al., 2011). Discharge of heavy metals into waters can occur directly and indirectly via anthropogenic and natural sources (Youzhi Li et al., 2020). Therefore, it is necessary to eliminate heavy metal ions from wastewaters and polluted waters.

Various methods such as membrane technologies (Pietrzak, 2013), nano-filtration (Mikulášek & Cuhorka, 2016), ion exchange (Dong et al., 2018), adsorption (Almasi et al., 2017b), electrocoagulation (Doggaz et al., 2019), chemical precipitation (Byambaa et al., 2018), coagulation/flocculation (CF) (Amuda et al., 2006), air floatation (Sun et al., 2020), phytoremediation (Jin et al., 2019), reverse osmosis (RO) (Thaçi & Gashi, 2019), solvent extraction (Konczyk et al., 2013), photocatalytic degradation (Dhandole et al., 2020), electrochemical technologies (El-Shafai et al., 2020), electro-dialysis (Nemati et al., 2017), modern radiation techniques (microwave) (Kiran et al., 2019), ultrasonic (Adeel et al., 2020), and advanced oxidation processes (AOPs) (Moersidik et al., 2020) have been used in the removal of heavy metals from aqueous solutions. As shown in Fig. 1, studies on the removal of HMs since 2010 have received considerable attention due to health and environmental hazards.

The results of previous research have confirmed that conventional water and wastewater treatment methods are unable to remove heavy metals according to established standards (Adeleye, 2016). Therefore, environmentalists need to develop novel methods to overcome the shortcomings of previous methods.

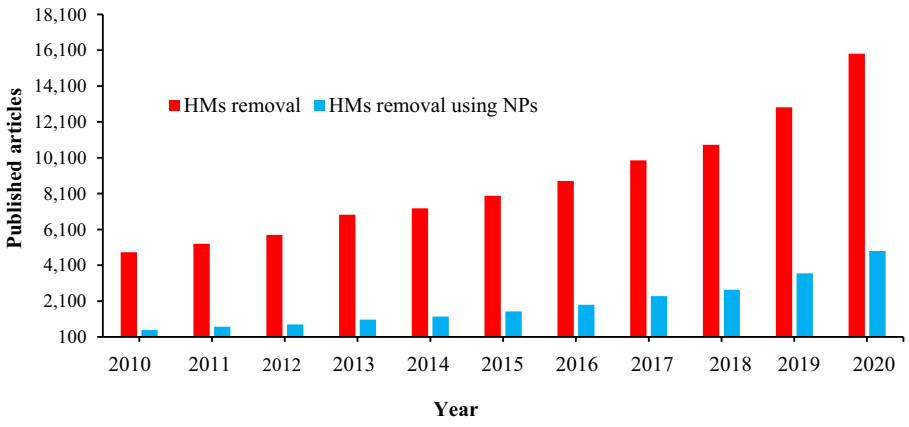

Fig. 1 The related published articles on the removal of heavy metals using conventional methods and nanoparticles (NPs) from 2010 to 2020

Among them, adsorption is an efficient and low-cost method in removing pollutants from water and wastewater due to the great removal efficiency, lack of sensitivity to toxic compounds, simple operation, high surface area, and high capacity (Almasi et al., 2017b; Nayeri et al., 2019; Shahbazi et al., 2020). The results of previous studies indicated that many factors such as surface area, functional groups of the adsorbent, physicochemical structure, dispersion stability, zeta potential of the adsorbent surface, pore size distribution, and polarity influence the adsorption efficiency (Chen et al., 2020; Mehdizadeh et al., 2014). Although adsorption process has numerous advantageous, the efficiency of this method can be restricted by mass transport resistance (Mehdizadeh et al., 2014). Therefore, researchers have attempted to introduce new adsorbents, namely nano-sized adsorbents (Di Natale et al., 2020; Gangadhar et al., 2012), to improve the efficiency of conventional adsorbents and overcome their shortcomings.

This new type of adsorbent has received considerable global attention for application in water and wastewater treatment because of the following advantages: high surface/volume ratio, amendable size and shape and biocompatible nature (Chaudhary et al., 2016), selective separation (Gómez Pastora et al., 2016), catalytic potential (Ebadi et al., 2016), ability to adsorb various metals (Farghali et al., 2013), high permeability, good sustainability (Gangadhar et al., 2012), having functional groups, absence of secondary wastes (Dil et al., 2019b; Farghali et al., 2013), high mechanical strength and high ordered structure (Nayeri & Mousavi, 2020a).

Nano-adsorbents can be classified into two main groups of inorganic and organic nano-sized adsorbents (Homaeigohar, 2020). Over the past decade, inorganic nano-adsorbents such as carbon nanotubes, nanocomposites, nano-clay, magnetic nanoparticles, metals oxides, and zero-valent iron have been developed to remove heavy metal ions from aqueous solutions (Fig. 1). Many single-faceted reviews have been published on the nano-adsorbents, but a comprehensive review of the recent development of inorganic nano-adsorbents for the removal of heavy metals is still lacking. Therefore, this work focuses on the application of inorganic nano-adsorbents for the removal of a wide range of heavy metals from the water systems. This paper presents general information regarding the sources and negative effects of heavy metals, the conventional methods of HMs removal, the concept and adsorption mechanism of HMs, and also the advantages and limitations of the different types of nano-adsorbent are evaluated. Other relevant realms and factors investigated in this paper include the following: developed inorganic-nanostructured adsorbents such as chemical and physical characteristics using various methods, namely Brunauer–Emmett–Teller (BET), Scanning Electron Microscope (SEM), Fourier-transform infrared spectroscopy (FTIR), X-ray diffraction analysis (XRD), evaluating the effect of operational factors on the removal efficiency such as initial metal concentration, pH, contact time, and nano-adsorbents dosage; reviewing various isotherm models (Langmuir, Freundlich, Temkin, Sips, and Dubinin–Radushkevich) and kinetic models (pseudo-first-order, pseudo-second-order, intraparticle diffusion, and Elovich) of the adsorption process, and finally negative effects of nanomaterials on the human health were discussed.

2 Sources of heavy metals

The heavy metals in the aqueous solutions are originated in two main sources: the natural source such as the pedogenetic and weathering processes and the human source such as agricultural, mining, industrial, and urban activities (Nguyen et al., 2020; Youzhi Li et al.,

2020). As, Cd, Cu, Co, Al, Cr, Ni, Mn, Hg, Pb, Sn, Zn, and Fe are some of the HMs that can be found in water and wastewater (Nguyen et al., 2020; Youzhi Li et al., 2020). Among them Cu, Pb, Zn, As, Cd, Cr, and Hg as primary control pollutants need more attention by environmental agencies and scientists (Pekey, 2006; Qiao et al., 2020). In brief, the sources of some of the more dangerous HMs, which can be founded in water and wastewater, were reported as follows:

Cadmium could be released in ecosystems by natural resources such as rock weathering, forest fires, and volcanic eruptions (Boparai et al., 2013). Anthropogenic activities such as waste incineration, metal electroplating, fertilizer production, polyvinyl chloride (PVC) products, cadmium alloys, and batteries are another source of cadmium component in water bodies (Abd El-Latif et al., 2013; Boparai et al., 2013).

Lead as an HM is generally combined with sulfur as galena (PbS), which is the main lead-bearing mineral (Fashola et al., 2016). Lead is used in batteries, dyes, paper, and pulp industries, mining, canning, lead smelting, metallurgy, tannery, cables, pesticides, steels and alloys, soundproofing materials, and other industrial and agricultural activities (Chaudhry et al., 2016; Fashola et al., 2016; Mousavi et al., 2019).

Mercury as Hg enters into the environment from natural and anthropogenic sources. Among the man-made sources are activities such as mining, barometer and thermometer production, pharmaceutical products (Yaghmaeian et al., 2015), electroplating, catalysts, thermometers, fluorescent light bulbs, barometers, batteries, electrical switches and relays, mercury lamps, semiconductor solar cells, and pharmaceuticals (Björkman et al., 2007; Park & Zheng, 2012).

Chromium is one of the most plentiful elements in the Earth's crust (Izbicki et al., 2008). This element is naturally adsorbed by grains, meats, and vegetables (Gautam et al., 2016). Furthermore, compounds of chromium could be found in industrial activities such as chromic acid and Cr pigments manufacturing, wood preservation, leather tanning, producing paints and dyes, printing products, oil refining, stainless steel production, textile manufacturing, and pulp production (Gaffer et al., 2017; Khatoon et al., 2013; Zandipak, 2017).

Arsenic components with an average terrestrial concentration of about 5 g/ton are naturally distributed in the Earth's crust (Langsch et al., 2012). The water systems can be polluted by arsenic due to gold mining, natural erosion, geochemical reactions, biological activity, volcanic eruption, and burning of fossil fuels (Mandal et al., 2013). This element is used in car batteries, paint and dyes, pesticides, textiles, medical wastes, semiconductor production, electronic industries, food additives, cement, and glass industry (Agrafioti et al., 2014; Pillai et al., 2020).

Nickel is a natural element in the earth's crust (Karnib et al., 2014). This element can be introduced in natural ecosystems from sources such as municipal waste incineration, mining, fuel burning, and residual oil burning, fly ashes, boilers, cement, pesticides, electroplating, porcelain enameling, and power plants (El-Sadaawy & Abdelwahab, 2014; Gautam et al., 2016).

Copper as a native metal can be found in nature in a usable form and has been widely used in electrical wire, plumbing, electronics, white goods, and in alloys such as brass, bronze because of special properties such as electrical conductivity and high corrosion resistance (Li et al., 2014; Tiwari et al., 2017). Furthermore, this element is used in nutritional supplements, electroplating, petroleum refining, mining, tannery, and many other products and activities (Demiral & Güngör, 2016; Elkady et al., 2015).

Cobalt has been used in pigments, rechargeable batteries, electric vehicles, high-performance alloys, mining, plating, metalworking, paints, and electronics (Tizro & Baseri, 2017).

Zinc is the most common metal ion in aqueous media and has had widespread application in various sectors (Ali et al., 2019). This metal is essential for the physiological function of living tissues and controls various biochemical processes (Farid et al., 2017). It can reach the environment and cause serious pollution through various ways such as paints, pigments, rubber and chemical industries, batteries, ammunition production, and electroplating (Jagaba et al., 2020; Omraei et al., 2011).

3 The effects of heavy metals on human health

The HMs from the aforementioned sources especially wastewaters find their way into the environment and contaminate receiving waters, soil, and groundwater and pose danger to all life forms (Abd El-Latif et al., 2013; Agrafioti et al., 2014). As they are non-biodegradable and cannot be metabolized, they engender bioaccumulation and bio-magnification in the food chain (Madala et al., 2017; Valentín-Reyes et al., 2019). Therefore, in this section, the effects of HMs on the human body and environment have been briefly discussed.

Cadmium can be enriched in agro-products (e.g., vegetables, and crops, and sea products like shellfish (Chunhabundit, 2016). The consumption of food containing this element results in poisoning, and it has negative effects on the nervous system, organs such as liver, lungs, and kidneys, and cardiovascular system via accumulation. Such accumulation can cause carcinogen-teratogen, laryngitis, asthma attacks, pulmonary fibrosis, acute gastrointestinal pain, and finally death (Table 1) (Madala et al., 2017; Trinh et al., 2019; Valentín-Reyes et al., 2019). The most remarkable cadmium toxification is Itai-Itai disease common in Japanese Jintsu River Valley, because of rice irrigation by contaminated water (Yoshida et al., 1999). Food and Agriculture Organization (FAO) and World Health Organization (WHO) reported that the maximum daily intake of cadmium from all sources (water, soil, and air) is 1–1.2 μg/kg of body weight (Kakaei, 2016). The maximum concentration of cadmium in drinking water is 0.003 mg/L as decided by WHO (Madala et al., 2017).

Lead is not an essential element and can be accumulated in human organs after uptake from food, air, or water (Pourrut et al., 2011). The results of studies have indicated that Pb will be effect on the different aspects including decrease of the intelligence quotient (IQ) in children, exacerbate mental and behavioral dysfunctions, causing high blood pressure, anemia, and headache, muscle aches, general fatigue and anger, compromise fertility in adults, trigger nervous system burnout, loss of memory, nausea, insomnia, anorexia, elevate the risk of developing Alzheimer's disease, and also reduction in the production of hemoglobin (Brooks et al., 2010; Manyangadze et al., 2020; Nayeria et al., 2019). Upon long-term exposure to lead, it can be replaced with calcium at the point of calcium release (bone tissue) and interfere with normal bone formation process (Brooks et al., 2010; Dixit et al., 2017; Ramesh et al., 2013). Table 1 shows the results of lead exposure in children. Due to these significant effects, the US Environmental Protection Agency (US. EPA) estimates the maximum lead concentration into the environment at 0.015 mg/L. WHO has reported the levels of lead in surface waters at less than 0.1 mg/L and non-polluted areas at 1 μg/L and below (Brooks et al., 2010; Dixit et al., 2017; Ramesh et al., 2013).

Mercury is a serious threat to human life and natural ecosystems because of its high toxicity (Park & Zheng, 2012). Hg can be found in the environment as mercuric (Hg^{2+}), mercurous (Hg^{+}), elemental (Hg^{o}), or alkylated form (methyl/ethyl mercury), which is the most toxic forms in water (Park & Zheng, 2012; Yaghmaeian et al., 2015). It can adversely affect tremors, insomnia, memory loss, and neurologic systems (Mahurpawar, 2015). The

Table 1 The events by exposure to HMs

Types	Year	Location	Effects	References
Cd	2009	Xinma Village, Zhuzhou City, Hunan Province	2 deaths and 150 chronic low-toxicity	Takahashi (2016)
Pb	2012	Dapu Town, Hangkong County, Hunan Province	300 children had more than 486 mg/L of lead in their blood	Takahashi (2016)
As	2014	Shimen City, Changde city, Hunan province	700 people were poisoned, which is thought to lead to cancer and 157 people die of poisoning	Mahmood (2012), Takahashi (2016)
As	–	Bangladesh	Killed 200,000–270,000 because of cancer	Gardner (2009), Mahmood, 2012)

most notable mercury occurrence is the Minamata disease, which is the result of discharging mercury sulfate from wastewater into the Minamata Bay and Shiranui Sea (Yokoyama, 2018). The mercury sulfate is metabolized to methylmercury by bacteria in the sediment, and this toxic chemical is bioaccumulated and biomagnified in the shellfish and fish and consequently in the human body (Barkay and Wagner-Döbler, 2005; Mahurpawar, 2015). Moreover, scientists reported that methylmercury triggers autism and learning disabilities (Leslie & Koger, 2011). Acute toxicity of mercury by exposure to mercury vapor during an accident at a fluorescent lamp is shown in Fig. 2 (Do et al., 2017). The U.S. EPA reported that the limit of the mercury discharge into wastewater is 10 µg/L and the maximum acceptable concentration in drinking water is 1 µg/L (Huang et al., 2016).

Chromium as chromite (Cr^{+3}) and chromate (Cr^{+6}) can be predominantly introduced into the environment through the aforementioned sources (Wang et al., 2020). Because of mutagenic characteristics, Cr^{+6} is listed as an anthropogenic human carcinogen (Group I) by the IARC (International Agency for Research on Cancer) (Huang et al., 2017; Leonard & Lauwerys, 1980). This element damages organs such as kidneys, and, liver and helps develop lung tumors, severe diarrhea, skin allergy, mucous membranes, respiratory problems, and internal bleeding (Mahurpawar, 2015). To reduce these health effects of chromium, the US. EPA has announced the allowable amount of dischargeable to surface water at below 0.05 mg/L (Liu et al., 2020a). In Fig. 2, an occurrence of chromium damage has been reported for a person who consumes polluted water (Thakare et al., 2017).

Arsenic can be associated with skin damage and hyperkeratosis at short-term exposure (Dastgiri et al., 2010). Long-term exposure to arsenic elevates the risk of cancer of skin,

Fig. 2 Effects of heavy metals on human health (Do et al., 2017; Jetty et al., 2013; Mandal et al., 2016; Sharquie et al., 2011; Thakare et al., 2017)

lungs, liver, kidneys, and bladder, and intestinal problems, thickening of the skin, blood vessel diseases, high blood pressure, reproductive disorders, and other non-carcinogenic diseases (Hernández-Flores et al., 2018; Mandal et al., 2013). Exposure to arsenic in the workplace by inhalation can also cause lung cancer and non-malignant skin changes such as keratosis (Fig. 2) (Mandal et al., 2013). Arsenic-polluted drinking water in Bangladesh killed 200,000 to 270,000 because of cancer (Gardner, 2009). Based on previous studies, 700 persons were poisoned, which is thought to lead to cancer, and 157 people died due to poisoning by exposing at high risk of water contaminated with arsenic (Table 1) (Gardner, 2009; Mahmood, 2012). WHO has considered 10 ppb as a permissible limit in drinking water (Chaudhry et al., 2017).

Nickel compounds are easily adsorbed at high concentrations and can cause lung, bone and respiratory tract cancer (Fonseca-Correa et al., 2019). In addition, acute Ni (II) poisoning leads to chest pain, rapid breathing, dermatitis, skin allergies cyanosis, and headache (Fonseca-Correa et al., 2019). Furthermore, nickel according to Fig. 2 can cause allergies and dermatitis (Jetty et al., 2013). The tolerance limit of nickel concentration in drinking water and industrial wastewater is 0.01 mg/L and 0.2–2 mg/L, respectively (Venkateswarlu et al., 2015).

Copper is a vital micronutrient for plants and animals, but at high concentrations it is toxic for all organisms (Hänsch & Mendel, 2009). At high concentrations in water, this element can cause diarrhea, vomiting, stomach cramps, dermatitis, asthma, bronchitis, anemia, kidney, and liver damages (Rachmawati et al., 2013). Therefore, the WHO recommends the maximum allowable concentration of copper in drinking water at 0.01 mg/L (Wehbe et al., 2020).

Cobalt in the environment can lead to many health problems such as low blood pressure, vomiting, nausea, heart disease, vision problems, loss of appetite, thyroid damage, hair loss, bleeding, diarrhea, and bone defects, and may also cause mutation (Tizro & Baseri, 2017).

Zinc has important roles in living organisms, including proper functioning of more than 200 enzymes, DNA stability, gene expression, and signal transduction across the nervous system (Larakeb et al., 2017; Manal & Leila, 2016). However, its high concentration causes negative effects such as gastroenteritis, peritonitis (peritoneal inflammation), growth retardation, stomach cramps, skin sensitivity, diarrhea, vomiting, anemia, shock, and ultimately death (Larakeb et al., 2017; Manal & Leila, 2016). WHO has been determined 3 ppm Zn as the maximum acceptable level in wastewater and drinking water (Ali et al., 2019).

Thallium as a toxic heavy metal can produce effects like mutagenicity, carcinogenicity, and teratogenicity especially that many of its compounds are soluble in water (Asadpour et al., 2016). Besides, exposure to thallium in the short term can cause hair loss and scalp alopecia (Fig. 2), skin lesions, and damage to the nervous system (Sharquie et al., 2011). The clinical features of short-term thalamic poisoning include nausea, vomiting, diarrhea, dysfunction in dental organs, and hyperkeratosis with hair loss in the sub-stage (Sharquie et al., 2011).

4 The removal of heavy metals

Heavy metals can be eliminated from aqueous solutions using physical and chemical methods. Earlier research has addressed the physical methods such as mechanical screening, magnetic separation, and electrostatic separation (Gunatilake, 2015). Chemical processes

such as ion exchange (Dong et al., 2018), precipitation (Gangadhar et al., 2012), flotation (Sun et al., 2020), adsorption (Almasi et al., 2017a), coagulation/flocculation (Amuda et al., 2006) are widely used in the removal of heavy metals. The advantages and disadvantages of different methods are summarized in Table 2.

The advantages of membrane filtration such as stability, low energy requirement, and high removal efficiency make it suitable for the removal of metals, but this process has limited applicability because of high maintenance costs, production difficulties, disposal of residual materials, and high pressure requirement (Tiwari et al., 2017; Xia et al., 2017). On the other hand, the ion exchange method has several advantages like metal recovery and selectivity (Zewail & Yousef, 2015), but is limited due to high costs, lack of recyclability, the requirement of pretreatment and saltwater production (Gangadhar et al., 2012; Imchuen et al., 2016). In chemical precipitation, metals can be removed by the addition of organic polymers, alum, lime, and iron salts, but the main limitations of this method are the production of a large amount of sludge, high-cost requires operation and maintenance, and high power requirement (Gangadhar et al., 2012; Team, 2010). Another method that is used for the removal of heavy metals is air floatation. In this method, the bubbles stick to heavy metals and move them to the surface; due to high processing capacity and fast operation, it can be conveniently used for heavy metals removal. Nevertheless, this method has some drawbacks such as difficulty in scum control and the production of excess salt in the effluent of air floatation (Sun et al., 2020). Moreover, this technology requires high initial capital cost for operation and maintenance (Rubio et al., 2002). A coagulation and flocculation process due to the rapid and efficient method, low energy consumption, relatively simple design, non-toxic method, and low cost is helpful in water and wastewater treatment for the removal of heavy metal (Nayeri & Mousavi, 2020b; Ozairi et al., 2020; Sun et al., 2020). However, previous studies verified that using coagulant especially alum can cause neuropathological diseases such as Alzheimer (Nayeri & Mousavi, 2020a). Moreover, adsorption results in the production of high-quality effluents in many cases, and many adsorption processes are reversible (Mahmoud et al., 2015). The adsorption process is widely used due to its flexibility, design simplicity, ease of operation, non-susceptibility to toxic contaminants, avoidance of toxic substances, recovery of adsorbents, and more efficient operation (Akpomie & Dawodu, 2015; Mousavi et al., 2020). However, many adsorbents are not effective because of release or high inactive surface, or issues such as economic unjustifiability and production of secondary waste. Furthermore, it is difficult to separate adsorbents from the treated water after the completion of the adsorption process (Khazaei et al., 2016; Pirbazari et al., 2014). Nowadays, nanoparticles have been widely studied for the removal of various pollutants specially the HMs in water and wastewater because of their outstanding properties such as high surface to volume ratio compared to conventional adsorbents, larger pore size, higher adsorption capacity, faster removal dynamics, and greater removal efficiency (Adeli et al., 2017).

5 Nano-adsorbent

In general, the sorption of water-soluble materials within a solid phase is called the adsorption process (Ali, 2012). Adsorption is a separation process in which some components of the fluid phase are transferred to the surface of a solid adsorbent. The adsorption of the transfer function from the liquid phase to the solid phase is widely used in the treatment of water and wastewater (Dowlatshahi et al., 2014). The adsorption of pollutants on the

Table 2 The removal methods of heavy metals from water and wastewater: Advantages and disadvantages

Technology	Disadvantages	Advantages	References
Ion exchange	High operation and maintenance costs, long lifetime regeneration	Ability to recover heavy metal ions from resin, high efficiency, simplicity, effectiveness, low cost, simple operation	Daud et al. (2015), Hekmatzadeh et al. (2012), Nur et al. (2015)
Membrane filtration	High operating costs and pressure maintenance	Low production of solid waste, low chemical consumption, selectivity to metals, high efficiency, ease of operation, selective properties, thermal resistance, chemical, and mechanical resistance	Andrade et al. (2017), Chougui et al. (2014)
Adsorption	High cost, lack of selectivity, not effective at very low concentrations	High capacity, fast, cost-effective, no sludge production, easy recovery, simplicity	Ghaniem et al. (2016); Kumar et al. (2017); Nadia Moustafa Ahmed (2015); Salam et al. (2011)
Reverse osmosis (RO)	High cost, high energy, relatively high pressure, electrical necessity, repeated erosion	High removal rate, effective, easy to use, easy operation, high purity of water quality	Belkacem et al. (2007); Wimalawansa (2013)
Chemical oxidation	Low stability	Simple and fast, minimal residual masses	Langsch et al. (2012)
Nanoparticles	Difficulty to separate, challenges in the recycling after the treatment	High surface, abundant functional groups, efficient, cost-effective, environment-friendly, simplification of the synthetic procedure, high sorption capacity, fast kinetic	Das et al. (2014); De Gisi et al. (2017); Gao et al. (2015); Hameed et al. (2016); Mthombeni et al. (2015); Venkateswarlu et al. (2019)

adsorbent surface requires several stages: (1) the transfer of the metal ion from solution to the adsorbent outer surface; (2) the transfer of contaminated mass to internal and porous adsorbent through diffusion; and (3) adsorption of adsorbate material on the adsorbent active sites (El-Kafrawy et al., 2017).

Nowadays nanoparticles have attracted much attention due to their distinctive physicochemical properties (Aldwayyan et al., 2013) as they are used in fields such as chemistry, physics, electricity, environmental engineering, medicine and biology (Gangadhar et al., 2012; Mohammed, 2015). The word "Nano" comes from the Greek word "Nanos" meaning "dwarfs" and refers to an entity of a magnitude of 10^{-9}. Nanoscience focuses on the study of atoms, molecules, and objects that have particle size of a nanoscale (Gangadhar et al., 2012). Particle size is a relatively important feature of particles in the adsorption of pollutants. Therefore, smaller particle size can further improve the efficiency of the process because of wider specific surface area (Dargahi et al., 2015). Nanoparticles are considered suitable for water purification applications due to properties such as surface magnitude, catalytic potential, high reactivity, and self-assembly potential (Amadi et al., 2021; Ebadi et al., 2016). Furthermore, nano-adsorbents are extremely efficient in water-soluble applications due to lack of internal diffusion resistance for fast adsorption of organic molecules and heavy metal ions (Ebadi et al., 2016). There are a number of criteria for the use of nanoparticles as adsorbents for the effective removal of heavy metal ions from wastewater: (1) non-toxicity; (2) relatively high and selective adsorption capacity for low concentrations of pollutants; (3) easy removal of the adsorbed materials onto the adsorbent surface; and (4) recoverability of adsorbents (Wang et al., 2012). In recent decades, many studies have been carried out on the nano-adsorbents from a variety of aspects. Various inorganic nanoparticles such as metal oxides, nanocomposites, carbon nanotubes, magnetic nanoparticles, nano-zero-valent iron, and nanoparticles of clay have been employed for the treatment of water solutions, and researchers have reported several advantages during the last two decades (Table 3).

6 Inorganic nano-adsorbents

6.1 Nano-metal oxide (NMOs)

6.1.1 Physicochemical characteristics

This type of nano-adsorbent is produced in various sizes and shapes (small particles and granules) which have high adsorption efficiency (Mahmoud et al., 2015; Ociński et al., 2016). Among the metal oxide nanoparticles, iron oxide (Wang et al., 2010), titanium oxide (Poursani et al., 2016), zinc oxide (Venkatesham et al., 2013), magnesium oxide (Dargahi et al., 2015), nickel oxide (Mahmoud et al., 2015), manganese oxide (Ghaniem et al., 2016), copper oxide (Farghali et al., 2013) and zirconium oxide have been studied (Chaudhry et al., 2017). Physical structure and chemical characterization of metal oxide nanoparticles have been analyzed in various studies through Brunauer–Emmett–Teller (BET), scanning electron microscope (SEM), and Fourier-transform infrared spectroscopy (FTIR) to determine the specific surface area, the pore size and the functional groups on the adsorbent surface (Abd El-Latif et al., 2013; Chaudhry et al., 2016). The physicochemical characteristics of various NMOs are summarized in Table 4. The specific surface area (S_{BET}) as a physical property determines the quality and adsorption potential of

Table 3 Advantages of various inorganic nanoparticles

Classification of NPs	Advantages	Reference
Carbon nanotubes	Unique electronic properties, interesting physicochemical properties, excellent thermal conductivity, high thermal stability, high surface area, mechanical strength, strong sorption ability	Dil et al. (2019a), Salam (2013)
Nanocomposite	High surface/volume ratio, can greatly enhance the properties of materials, increasing the strength of materials and corrosion resistance, easy manufacturing, superior mechanical properties, structural and thermal stability	Julkapli et al. (2015), Okpala (2014)
Nano-clay	Enhance polymer mechanical, cheap and nonhazardous, high surface, high stability	Meira et al. (2015), Salam et al. (2017)
Magnetic NPs	Few productions of secondary wastes, large active surface area, high magnetic properties, high adsorption efficiency, easy and rapid separation	Giraldo et al. (2013), Keyhanian et al. (2016)
Metals oxides NPs	Large surface areas, high activities, cost-efficient water and wastewater treatment	Farghali et al. (2013)
Zero-valent iron	Easily accessible, generates very little waste and secondary pollutants, great ability to reduce and stabilize different types of ions, the high uptake capacity, high surface area, lower cost, non-toxic, high reactivity	Bhowmick et al. (2014), Esquinas-Requena et al. (2020), Kumar et al. (2017), Oprčkal et al. (2017), Üzüm et al. (2008)

Table 4 The NMOs' characteristics

NMOs	S_{BET} (m^2/g)	SEM/FESEM	FTIR	XRD	References
Zinc oxide	80.42	All the particles are regular and are flake-like	–	Crystalline morphology	Venkatesham et al. (2013)
Nickel oxide	128.33	–	Ni–O stretching vibration: 400–850 cm^{-1}, O–H stretching vibrations: 3357.9 and 3347.4 cm^{-1}, H–O–H bending vibration: 1621.8 and 1616.6 cm^{-1}	Purity and crystalline structures	Mahmoud et al. (2015)
Manganese oxides	91.97	Particles are uniformly distributed and mainly composed of spherical particles with 20 nm of average grain size	O–H vibrating: 3398, 1662, 1536 and 1390 cm^{-1}, metal–oxygen (Mn–O) bending vibration in δ-MnO_2: 617 cm^{-1}, metal–oxygen (Mn–O) bending vibration of [MnO_6]: 514 cm^{-1}	The mixture of different phases such as MnO, MnO_2, and Mn_3O_4	Ghaniem et al. (2016)
Titanium dioxide	55.35	–	Stretching bands of adsorbed water: 3446 cm^{-1}, hydroxyl bond: 1635 cm^{-1}, Ti–O-N bond: 1031 cm^{-1}, vibration of titanium and oxygen bonds and anatase form of TiO_2: 455 cm^{-1}	Crystalline morphology	Poursani et al. (2016)
Nickel-oxide	–	Particles were agglomerated, randomly shaped, and multi dispersed	Ni–O bond: 411 cm^{-1}, O-C=O and the C–O stretching vibration: 1000–1500 cm^{-1}, band O–H stretching vibrations: 3440 cm^{-1}, H–O–H bending vibrations: 1635 cm^{-1}	Crystallite size	Panji et al. (2016)
Magnesium oxide	High surface area	The powder is porous and agglomerated	Stretching vibration mode for Mg – O: 520 cm^{-1}, O–H bending: 1500 and 3500 cm^{-1}	Well crystallized	Madzokere and Karthigeyan (2017)

nano-adsorbents (Poursani et al., 2016). As can be seen, the S_{BET} of NMOs varies from 55.35 to 128.33 m^2/g (Mahmoud et al., 2015; Poursani et al., 2016). Based on Table 4, SEM is another important test, which has been applied to characterize various NMOs. According to SEM results, it can be observed that the synthesized powder of NMOs approximately has agglomerated, spherical, regular, and uniformly distributed particles randomly shaped on the surface of adsorbents. Most NMOs have a size ranging from 20 to 70 nm (Ghaniem et al., 2016; Madzokere & Karthigeyan, 2017; Panji et al., 2016; Poursani et al., 2016; Venkatesham et al., 2013). It is well known that NMOs have different functional groups. Major functional groups of NMOs may be described as follows: (1) broad peaks at 1390, 1500, 1536, 1635, 1662, 3398, and 3500 cm^{-1} as contributed to hydroxyl bond (O–H); (2) O–H stretching vibrations observed at 3357.9, 3347.4, and 3440 cm^{-1}; (3) the peaks at 1621.8, 1616.6, and 1635 cm^{-1} probably being due to H–O–H bending vibration; and (4) Ni–O stretching vibration being detected at 400, 411, and 850 cm^{-1} (Ghaniem et al., 2016; Madzokere & Karthigeyan, 2017; Mahmoud et al., 2015; Panji et al., 2016; Poursani et al., 2016; Venkatesham et al., 2013). Moreover, the results of X-ray diffraction (XRD) analysis revealed that most NMOs have crystallite size (Ghaniem et al., 2016; Madzokere & Karthigeyan, 2017; Mahmoud et al., 2015; Panji et al., 2016; Poursani et al., 2016; Venkatesham et al., 2013).

6.1.2 Performance and the effect of variables

The efficiency of NMOs and the effects of environmental and process factors on the removal of pollutants have been investigated during previous studies. The identification of the effects of factors and their optimization are of particular importance in the application of this treatment method. The adsorbent dosage, initial concentration of metals, contact time, and pH are the most important parameters discussed briefly below. The adsorbent dosage can greatly affect the adsorption process and the adsorption capacity (Pirbazari et al., 2014). It also determines the capacity of an adsorbent according to the initial concentration of the adsorbent materials (Abd El-Latif et al., 2013). The results of the experiments show that increasing the adsorbent dosage proportionally raises the removal percentage because more sites are available for adsorption (Aljeboree et al., 2017).

A number of studies have investigated the effect of NMOs dosage. Taman et al. (2015) employed copper oxide nanoparticles for eliminating two heavy metals (Fe^{3+} and Cd^{2+}) from the wastewater. In this study, nano-adsorbent dosage varied from 0.1 to 0.4 g/L. It was found that higher dosage of 0.4 g/L enhances the removal efficiency of two heavy metals (Taman et al., 2015). The results of a similar study by Nadia Moustafa Ahmed (2015) showed that larger adsorbent dosage of ZnO nano-adsorbent from 2 to 10 g/L augmented the removal percentage of chromium (VI) from 45 to 53% but further increase in the dosage to higher than 10 g/L kept the efficiency of the system almost constant (Nadia Moustafa Ahmed, 2015). Madzokere and Karthigeyan (2017) synthesized the nano-adsorbent of magnesium metal oxide as an effective adsorbent for removing copper from an aqueous solution. They concluded the removal efficiency of copper from 30 to 96% by increasing the dosage to 2 g/L (Madzokere & Karthigeyan, 2017).

The initial concentration of heavy metals is a key parameter in adsorption efficiency. Previous studies have shown that the removal efficiency of metals was lowered as the initial concentration of heavy metals increased (Abd El-Latif et al., 2013). At the beginning of the adsorption process, there are wider adsorption sites on the surface of nano-adsorbent which can adsorb metals, but with increasing the concentration of metals, the number of active

sites is not sufficient and hence lower metal removal efficiency (Akpomie & Dawodu, 2015). This phenomenon can be attributed to the reduction of intermolecular forces and possibly the low solubility of nanoparticles at high concentrations of a metal solution (Dargahi et al., 2015). Salem et al. (2017) investigated the effect of the initial concentration of trivalent chromium ions, nickel, and cobalt on the removal efficiency of these metals using zinc oxide nanoparticles. The results showed that by increasing the initial concentration of metals, the percentage of metal adsorption by the nano-adsorbent reduced. These results can be associated with a reduction in ZnO active sites due to higher concentration of metals so that by increasing initial concentration, the active sites of ZnO become progressively blocked and the adsorption percentage of metal ions decrease consequently (Salem et al., 2017). The study by Bhakta and Munekage (2011) shows that at the dosage of manganese oxide of 0.05 g/L, the contact time of 24 h, and pH 7, by increasing mercury concentration, the removal efficiency also increased (Bhakta & Munekage, 2011).

Another parameter affecting the adsorption process is the contact time; therefore, to obtain the best condition for reducing costs, it is necessary to optimize this factor (Zandipak, 2017). The results of previous studies indicate that adsorption is the fastest at the early stages due to the presence of unsaturated active sites on the adsorbent surface (Akpomie & Dawodu, 2015). In addition, contact time can affect the interactions between adsorbent and adsorbate. Panji et al. (2016) used nickel oxide nanoparticles for removing heavy metals (chromium, copper, and nickel) from synthetic solutions with dosage of 60–140 mg/L for Cu and 100–700 mg/L for Cr and Ni. The results confirmed that by extending the contact time from 5 to 10 min, the removal efficiency increased, but by further increase in the contact time, the removal efficiency of chromium, copper, and nickel decreased. In the first 10 min of the contact time, the copper removal efficiency was about 94%, and the six-valent chromium was about 33.3%. The optimal time for the removal of nickel was approximately 97% in about 5 min (Panji et al., 2016). Fargha et al. (2013) used copper oxide nanoparticles to remove lead metal, and it was observed that as the contact time increases, the maximum adsorption is enhanced too. The maximum adsorption occurs in 4 h, and after that, no more adsorption is carried out (Farghali et al., 2013). Ali et al. (2017) confirmed that the removal efficiency of quaternary chromium increased when contact time increased from 10 to 60 min under constant conditions (guar gum–nano-zinc oxide biocomposite (1 g/L) and chromium concentration of 25 mg/L. The time of 50 min was selected as the equilibrium time of the process. Furthermore, the maximum removal percentage was 96.5% under the mentioned conditions (Ali et al., 2017).

Numerous works considered pH as an important parameter affecting the removal of heavy metals from aqueous solutions and stated that the pH value is related to the chemistry of metal in solutions and the ionization status of adsorbent groups that affects site accessibility (Al-Qahtani, 2016). Therefore, to investigate the effect of the acidic and alkaline conditions of solutions on the adsorption, experiments were performed on a wide range of initial pH values (Ghorbani et al., 2012). At low levels of pH, the solution is highly acidic and the adsorption surface is surrounded by hydrogen ions; therefore, due to the competition between hydrogen ions and metal ions, the removal percentage is low (Golkhah et al., 2017). Farghali et al. (2013) applied copper oxide to remove heavy metal at a different value of pH (3 to 6.5), and it was observed that by increasing the pH, the removal efficiency of the metal also increased, while the pH of 6.5 was at an optimal value (Farghali et al., 2013). Taffarel and Rubio (2010) studied the removal efficiency of Mn^{2+} from aqueous solution using manganese oxide-zeolite with varied dosage (1–6 g/L). They found that the adsorption of Mn^{2+} ion was enhanced with increasing pH from 4 to 8 (Taffarel & Rubio, 2010). The results of a

study by Panji et al. (2016), which has been carried out on the removal efficiency of Cr (VI), Cu (II), and Ni (II), indicated that the efficiency of the system was strongly dependent on the pH value. The adsorption of Cu (II) and Ni (II) was improved by elevating the pH from 3 to 11, with the removal efficiency of 99.1% and 98.3%, respectively, but the maximum removal of chromium (VI) occurred at acidic pH of 3 (Panji et al., 2016).

6.2 Nanocomposites (NCs)

6.2.1 Physicochemical characteristics

The nanocomposite is a multiphase material in which one of its phases is less than 100 nm in one, two, or three dimensions or its structures have duplicate spacing within the nano-range in different phases of the substance (Singh et al., 2014). Nanocomposites have been developed as a critical water purification technique because of outstanding properties such as better performance in desalination processes, favorable material separation, and thermal stability (Atta et al., 2016). The other category is a nano-sized composite polymer that created a new potential for composite materials by introducing a small number of nanoparticles to the polymers. This type of polymeric NCs has drawn significant interest in recent years due to their research and industrial value (Singh et al., 2014). This new and reliable nanomaterial present excellent mechanical strength with high adsorption performance of various pollutants that can retain their inherent properties (Azad et al., 2021). NCs have various configurations and physical and chemical characteristics as scrutinized in earlier research. For determining the morphology and chemical structure of nanocomposites, different approaches have been adopted such as BET, FESEM, SEM, XRD, FTIR, X-ray photoelectron spectrometry (XPS), vibrating-sample magnetometer (VSM), and thermogravimetric analysis (TGA) (Abd El-Latif et al., 2013; Choudhury et al., 2015; Wang et al., 2010). The characteristics of NCs, with a range of S_{BET} from 17.31 m^2/g (zeolite/ZnO) to 1737.62 m^2/g (Fe_3O_4 magnetic polypyrrole–graphene oxide) (Alswata et al., 2017; Zhou et al., 2017), used for eliminating HMs from aqueous solution, are illustrated in Table 5. It is shown that NCs are reliable adsorbents for HMs removal. As seen in Table 5, many functional groups on the nanocomposite surface have been detected, the most important of which are as follows: (a) hydroxyl group (O–H) can be ascribed at peak 1648, 3132.8, 3349,3418.9,3630, 3627 cm^{-1}; (b) vibration of the bond Si–O-Si is attributed to 459, 466, 548, and 935 cm^{-1}; and (c) the vibration of the Si–OH group can appear at peaks 965 and 3434 cm^{1} (Alswata et al., 2017; Choudhury et al., 2015; Shafiabadi et al., 2016; Zhou et al., 2017). According to Table 5, by SEM analysis, it can be concluded that NCs have a varying surface morphology because of using different NCs for removing HMs. Zhou et al. (2017) reported that nanocomposite of Fe_3O_4 magnetic polypyrrole–graphene oxide had a cauliflower-like and granular morphology on the surface (Zhou et al., 2017). A similar study by Alswata et al. (2017) has confirmed that zeolite/ZnO nanocomposite had granular shapes on the adsorbent (Alswata et al., 2017). The morphological results of El-Latif et al. (2013) and Choudhury et al. (2015) revealed that the surface of NCs is uniformly spherical and porous, as utilized for the removal of cadmium and lead (Abd El-Latif et al., 2013; Choudhury et al., 2015). Based on XRD results, it can be understood that most NCs have crystalline structures (Abd El-Latif et al., 2013; Alswata et al., 2017; Choudhury et al., 2015; Diva et al., 2017; Shafiabadi et al., 2016; Zhou et al., 2017).

Table 5 The NCs' characteristics

NCs	S_{BET} (m^2/g)	SEM/FESEM	FTIR	XRD	References
Fe_3O_4 magnetic polypyrrole–graphene oxide	1737.6	Nanocomposite had a cauliflower-like and granular morphology	The vibration of hydroxyl: 3132.8 and 3418.9 cm^{-1}, carbonyl and carboxyl groups (C=O): 1713.5 and 1633.2 cm^{-1}, C=C bonds in the GO and Py rings, respectively: 1600.1 and 1540.3 cm^{-1}	Crystalline structures	Zhou et al. (2017)
Zeolite/ZnO	17.31	The surface of zeolite/ZnO NCs has granular shapes	O–H stretching: 3349 and 1648 cm^{-1}, stretching vibration of Si–O: 965 cm^{-1}, Si–O–Si bending vibration: 548–459 cm^{-1}, ZnO NPs and Zn–O bond in the ZnO NPs: 357 to 353 cm^{-1}	Zeolite crystalline structure in the presence of ZnO NPs	Alswata et al. (2017)
Bentonite clay-based hydroxyapatite NCs cross-linked by glutaraldehyde	21.89	Signifies the formation of nearly uniform spherical HAp NPs The porous surface of the NCs was also confirmed	Hydroxyl group (–OH): 3627–3630 cm^{-1}, Si–O–Si bonds: 1040–1044 cm^{-1}, $-PO_4$ groups: 1036 to 1043 cm^{-1}	Crystalline structure	Choudhury et al. (2015)
Alumina-Iron Oxide	298	The particles are nearly uniformly spherical, and the particle size can be measured in the range of 25–29 nm	–	Crystalline structure	Abd El-Latif et al. (2013)

Table 5 (continued)

NCs	S_{BET} (m^2/g)	SEM/FESEM	FTIR	XRD	References
Polypyrrole/SBA-15	97.6	The PPy polymerization was occurred not only insides the pores, but also outside the SBA-15	The symmetrical vibrations and antisymmetric of Si–O–Si bond: 788 and 1099 cm^{-1}, the torsion vibration of the bond Si–O–Si and the vibration of the Si–OH group, respectively: 466, 935 and 3434 cm^{-1}, stretching vibration of C–H: 2918 cm^{-1}, C–N stretching vibration: 2356 cm^{-1}, C=C ring stretching of pyrrole: 1635 cm^{-1}, C–H vibrations 1305 cm^{-1}	Hexagonal structure	Shafiabadi et al. (2016)
Nickel oxide/CNT	90	NiO nano-crystallites are aggregated, forming clusters with larger grains	–	Crystallographic	Diva et al. (2017)
Activated SiO_2@C	262.39	The milled SiO2@C prepared by burning the husk in ambient atmosphere (SC1) exhibits spherical grain morphology with the grain sizes ranging between 20 and 50 nm	O–H vibrational stretching of OH group or adsorbed-water: 3425 cm^{-1}, C–H vibrational stretching of CH_2 group: 2925 and 2850 cm^{-1}, the vibrational stretching of C=O for ketone, aldehyde, lactone, or carboxyl groups: 1705 cm^{-1}, the aromatic-rings or vibrational stretching of C=C: 1700 and 1605 cm^{-1}, the vibrational bending of CH_3: 1375 and 1450 cm^{-1}	Amorphous	Zawrah and Alhogbi (2021)

6.2.2 Performance and the effect of variables

A parameter on the efficiency of nanocomposite is the adsorbent dosage, which has been studied in many works. The results have confirmed that an initial increase in the removal efficiency (by adsorbent dosage increment) is due to a creating larger surface area as well as more available adsorption sites (Alswata et al., 2017). It has been mentioned that the adsorption capacity and the increase in the adsorbent dosage have an inverse relationship so that the adsorption capacity is reduced as the adsorbent dosage rises (Farooghi et al., 2018). Furthermore, studies have demonstrated that the quantity of adsorbent is used to describe the adsorbent cost per unit volume of solution, which is considered for treatment (Zare et al., 2016). Alswata et al. (2017) used zeolite/zinc oxide NCs for the removal of Pb (II) and As (V) metals from aqueous solution, and it was observed that by increasing the amount of adsorbent dosage from 0.2 to 3 g/L, the adsorption of two heavy metals was also elevated from 38.9 to 90.8% and from 52 to 85.5%, respectively. In this study, optimal parameters for removal of toxic metals were 93% and 89% for Pb (II) and As (V) at 100 mg/L, pH 4, the adsorbent dosage of 3 g/L, and contact time of 30 min (Alswata et al., 2017). Tizro and Baseri (2017) studied the cobalt removal from aqueous solution using NCs based on magnetic properties. They found that the removal efficiency rose upon increasing the amount of adsorbent dosage, due to larger number of available sites on the adsorbent (Tizro & Baseri, 2017). Dahaghin et al. (2017) employed Fe_3O_4@graphene oxide nanocomposite modified with 2-mercaptobenzothiazole as an adsorbent for the elimination of heavy metals (copper, lead, and cadmium). In this study, the dosage of nano-adsorbent varied from 5 to 30 mg/L. They found that adsorbent dosage had a positive effect on the efficiency of the system so that by increasing the nano-adsorbent dosage from 5 to 15 mg/L, the efficiency of heavy metals was also boosted to 100% (Dahaghin et al., 2017).

Another important factor affecting the adsorption process is the pH value. It has been stated that at low pH values (acidic pH), hydronium ions are accumulated on the surface of the adsorbent, which leads to competition with metal ions and reduces the efficient adsorption process. At higher pH levels (alkaline pH), because of a reduction in the number of hydronium ions on the adsorbent surface, more metals can be adsorbed (Shahriari et al., 2014). In addition, pH has a significant effect on the removal of metal ions from aqueous solutions, which affects the metal chemistry in the solution and the ionization status of adsorbing agent groups on accessible binding sites (Huang et al., 2015). Previous research studies indicated that when pH value increases, even higher than point of zero charge (pH_{PZC}), deprotonation brings back the negative charge for functional groups (Ma et al., 2019). Farooghi et al. (2018) investigated the effect of the varied pH (3–8) for the removal of lead metal using $FeNi_3$@SiO_2 magnetic NCs, and it was observed that by increasing pH from 3 to 6, the removal efficiency was increased and the optimal pH value was selected at 6 (Farooghi et al., 2018). Molaei et al. (2017) revealed that the removal efficiency of five types of HMs (copper, lead, zinc, chromium, and cadmium) increased as the pH value was elevated from 4 to 7 due to the depletion of the nano-sorbent surface from protons but further increase leads to a decline in the removal efficiency of HMs (Molaei et al., 2017).

Many efforts have been made to understand the effect of initial concentration of pollutants on the adsorption process, and it has been concluded that the initial concentration of metal is a major driving force to overcome the resistance of metallic mass transfer between the aqueous phase and the solid phase (Shaibu et al., 2014). It should

be noted that at higher initial concentrations, the number of metal ions is greater than active adsorption sites; therefore, the removal efficiency is lessened at higher initial concentration (Diva et al., 2017). Diva et al. (2017) used nickel oxide-CNT nanocomposites for the elimination of HMs from aqueous solution and the initial concentration of the metal ranged from 20 to 100 mg/L. The results of the study demonstrated that at higher initial concentration of metal, removal efficiency decreased, and the concentration of 20 mg/L was selected as optimal (Diva et al., 2017). Li et al. (2019) investigated the feasibility of nano-composites Mn_3O_4@reduced graphene oxide for the removal of uranyl. They concluded that by increasing the initial concentration of uranyl from 0 to 20 mg/L at temperature of 298 K, ionic strength of 0.01 M and pH equal to 5, the adsorption capacity of uranyl also was boosted to higher than 120 mg/g (Li et al., 2019). Besides, Pradhan et al. (2017) investigated the effect of different initial concentrations of chromium and copper ions (100–1000 mg/L) in wastewater using silver-yttrium oxide nanocomposite. The results showed that increasing the initial concentration had a reverse effect on the removal efficiency of both metals from wastewater so that the removal efficiency of copper and chromium declined from 38.6 to 30%, and 38.4 to 29.36%, respectively (Pradhan et al., 2017).

Contact time as the most effective adsorption parameter has been widely investigated in previous studies. Ions are quickly removed at the onset of the adsorption process, but it will decrease with further extending the contact time because a large number of active adsorbent sites will be saturated at longer contact time, and therefore, the efficiency of the system will be reduced (Dehghani et al., 2015). In a study conducted by Shafiabadi et al. (2016) for the removal of mercury metal from aqueous solution using polypyrrole/SBA-15 nanocomposite, it was observed that, as the contact time was lengthened, the removal efficiency was increased accordingly (Shafiabadi et al., 2016). In another study, the removal of lead metal using $FeNi_3$@ SiO_2 magnetic nanocomposite was studied by Farooghi et al. (2018), and the contact time varied from 5 to 60 min. They found that by stretching the contact time, the elimination efficiency also increased (Farooghi et al., 2018). Ge et al. (2018) investigated the effect of contact time ranging from 0 to 120 min on the removal efficiency and adsorption capacity of lead metal using Fe@MgO magnetic NC. The results of the study showed that the lead metal was quickly adsorbed in the first 30 min and then reached equilibrium value in 120 min with 98.7% of adsorption, and the adsorption capacity of lead was 1476.4 mg/g of adsorbent (Ge et al., 2018).

6.3 Magnetic nanoparticles (MNPs)

6.3.1 Physicochemical characteristics

Over the past few years, magnetite nanoparticles (Fe_3O_4 NPs) have gained momentum in environmental engineering due to outstanding properties such as great performance, cost-effectiveness, high adsorption, being environmentally friendly, their excellent stability, recyclability, reusability, high capacity, and simple handling (Bekhit et al., 2020). Furthermore, it has been reported that the two commonly used MNPs in the crystalline phases are magnetite (Fe_3O_4) and maghemite (γ-Fe_2O_3), which have a high surface area, and eventually can be easily separated from aqueous solutions by an external magnet; therefore, it can be widely used for the adsorption of many environmental pollutants like HMs (Pardo et al., 2021; Wang et al., 2010).

Nano-zero-valent Iron (NZVI) is another category of MNPs, which has been recently successfully used to extract heavy metals, and quick separation potential from the aqueous solution by magnetism is a main property of this NP (Agarwal & Patel, 2015). NZVI due to its specific properties, including high reactivity, non-toxic catalytic properties, and low production cost attract considerable attention for environmental remediation (Akbari & Mohamadzadeh, 2012; Huang et al., 2015).

The physicochemical structure of the magnetic nanoparticles can be analyzed through various methods such as BET, SEM, FTIR (Khodadadi et al., 2015; Madivoli et al., 2016). To better scrutinize MNPs characteristics, the results of various studies that used MNPs for the HMs removal are summarized in Table 6. As can be observed, studies confirmed that MNPs have different S_{BET}, and among them, Fe_3O_4@SiO_2 core–shell MNPs have the highest S_{BET} of 216.2 m^2/g (Wang et al., 2010). Moreover, based on Table 6, studies have attested that the MNPs have numerous functional groups on the surface, the most important of which are as follows: there is an obvious broad peak around 585, 565,589, and 595 cm^{-1}, corresponding to stretching vibration of Fe–O; the peak at 2924, 2945, and 2522 cm^{-1} revealed the presence of C–H stretching, the C=O show a stretching vibration at 1642 cm^{-1}, the peak at 2924, 1563, 1642 cm^{-1} are related to stretching vibration of C–H, C–N, and C=O, respectively (Ahmad et al., 2019; Gao et al., 2015; Shirsath & Shirivastava, 2015; Venkateswarlu et al., 2019; Wang et al., 2010). According to XRD results of some previous works, the structure of MNPs is crystalline with an inverse cubic spinel structure (Ahmad et al., 2019; Venkateswarlu et al., 2019; Wang et al., 2010). However, the results of a study by Liu et al., (2020a, 2020b) indicated the broad and flat amorphous diffraction peaks other than sharp crystalline diffraction ones (Liu et al., 2020b).

The physicochemical characteristics of various NZVI such as BET, SEM, FTIR, and XRD are also discussed in Table 6. As indicated, the S_{BET} of pristine NZVI varied from 14.2 and 5.64 m^2/g for NZVI and also 44.57 m^2/g for modified NZVI with granular red mud (Du et al., 2019; Üzüm et al., 2008; Zarime et al., 2018). Moreover, the results of surface morphological of NZVI demonstrated that the particles of the prepared nano-adsorbents are uniform in size, tight, and globular—spherical in shape; furthermore, it has mentioned that fresh iron particles appear to have size distribution within 20–80 nm (Akbari & Mohamadzadeh, 2012; Du et al., 2019; Üzüm et al., 2008; Zarime et al., 2018). Besides, based on Table 6, the major functional groups of NZVI are as follows: O–H stretching vibration appeared at 3415 and 3412 cm^{-1}, hydroxyl group, and nitro agent groups were detected at 3412 and 1320 cm^{-1}, respectively. Stretching modes of OH groups observed at 3000 to 3600 cm^{-1}, and the peaks at 1419, 2922, and 1002 cm^{-1} are related to –COOH stretching vibration, $–CH_2$ stretching of an aliphatic compound, and Si–O–Si in silicate groups, respectively (Akbari & Mohamadzadeh, 2012; Du et al., 2019; Zarime et al., 2018).

6.3.2 Performance and the effect of variables

The effect of the adsorbent dosage on the efficiency of metal removal showed that the removal efficiency initially increases and will be constant or slightly decreased after reaching the maximum adsorption value (Padmavathy et al., 2016). Studies on the effect of adsorbent dosage ultimately concluded that higher adsorbent dosage due to larger number of accessible surfaces for adsorption enhances the adsorption efficiency; however, after the maximum removal at the special dosage, the higher adsorbent dosage shows no effect on the process efficiency (Gupta et al., 2016). Nevertheless, it has been

Table 6 The characteristics of MNPs and NZVI

Class	NPs type	BET (m^2/g)	SEM/FESEM	FTIR	XRD	References
MNPs	Fe_3O_4 MNPs	–	Before adsorption shows the fine uniform nano-sized surface area and change in the uniform structure after adsorption has occurred	Fe–O bond: 589 cm^{-1}, Fe–O bond of bulk Fe_3O_4 was at 599 and 375 cm^{-1}	Magnetic nano adsorbent was pure Fe_3O_4	Shirsath and Shirivastava (2015)
	Poly (maleic anhydride)-graft-poly(vinyl alcohol) comb polymer-functionalized MNPs	71.33	Higher dispersion was achieved after modification by polymers	–	Broad and flat amorphous diffraction peaks other than sharp crystalline diffraction peaks were observed	Liu et al. (2020b)
	Magnetic amine-functionalized polyacrylic acid-nano-magnetite	69.90	Changes into particulate again with an average diameter of 20.1 nm	Stretching vibration and bending vibration of N–H: 419 and 1320 cm^{-1}, C–H stretching vibration: 2924 cm^{-1}, C–N stretching vibration: 1563 cm^{-1}, C=O stretching vibration: 1642 cm^{-1}	–	Gao et al. (2015)
	MNPs- SiO_2	–	MNPs are homogenized and spherical in shape The spherical in the shape of silica-coated MNPs	Stretching vibration of Fe–O: 595 cm^{-1}, Si–OH bond: 1095.9 cm^{-1}, –COOH: 1680 cm^{-1}	Crystalline in nature	Ahmad et al. (2019)

Table 6 (continued)

Class	NPs type	BET (m^2/g)	SEM/FESEM	FTIR	XRD	References
	Fe_3O_4- magnetic nanorods	10.88	-	O–H stretching vibrations: 3580 cm^{-1}, C–H stretching vibration of methyl and methoxy groups: 2925 to 2815 cm^{-1}, C–O stretching of acid groups: 1310 cm^{-1}, Fe–O at 585 cm^{-1}, C–H stretching: 2945 and 2522 cm^{-1}	The cubic inverse spinel structure	Venkateswarlu et al. (2019)
	Fe_3O_4@SiO_2 core–shell MNPs	216.2	–	Fe–O vibration: 565 cm^{-1}, stretching and bending vibrations of amino groups: 3361, 1572, 1498, and 692 cm^{-1}, stretching vibration of methylene groups of Fe_3O_4@SiO_2 –NH_2: 2800–3025 cm^{-1}	Crystalline structure	Wang et al. (2010)
NZVI	Montmorillonite- NZVI	36.97	The agglomeration expectedly declined with the increase of dispersion of nZVI when Mt was employed	–	The layer structure of Mt can serve as a perfect host for nZVI, which hereby also increases the stability of the NZVI particle	Bhowmick et al. (2014)
	NZVI -Diethylene Triamine Penta Acetic Acid	–	Particles were uniform in size and spherical in shape	Hydroxyl group: 3412 cm^{-1}, nitro agent groups: 1320 cm^{-1}	Crystal structure	Akbari and Mohamadzadeh (2012)
	NZVI	14.2	Fresh iron particles appear to have size distribution within 20–80 nm	–	Iron is mainly in its Fe^0 state	Üzüm et al. (2008)

Table 6 (continued)

Class	NPs type	BET (m^2/g)	SEM/FESEM	FTIR	XRD	References
	NZVI	5.64	Globular shapes, embedded and dispersed well in a layer of flaky bentonite	Molecular H_2O: 1645 cm^{-1}, stretching modes of OH groups: 3000 to 3600 cm^{-1}	The presence of elements FeO (α-FeO) was detected	Zarime et al. (2018)
	Granular red mud – NZVI	44.57	The particle surface is tight and a part of the fibrous maize straw exited in GRM	O–H stretching vibration: 3415 cm^{1}, O–H bending vibration: 1637 cm^{1}, –COOH stretching vibration: 1419 cm^{-1}, $–CH_2$ stretching of aliphatic compound: 2922 cm^{-1}, Si–O–Si in silicate groups: 1002 cm^{-1}	Iron oxide was reduced to ZVI by solid-phase reduction	Du et al. (2019)

reported that by increasing the adsorbent dosage, the adsorption capacity is reduced. This may be due to a decrease in the level of accessible surface for metal ions due to the overlap or accumulation of adsorption sites (Akpomie & Dawodu, 2015). Researchers reported that the enhancement in the removal of pollutants occurs as a result of the larger number of active sites, but then its value will be fixed (Adeli et al., 2017). Tizro and Baseri (2016) remove Pb (II) and Cu (II) metals by an Fe_3O_4 magnetic nanoscale adsorbent, and it was observed that by increasing the adsorbent dosage to 0.2 g the removal efficiency of metals was improved (Tizro & Baseri, 2016). Similar results have been reported by Tizro and Baseri (2017), which investigated the cobalt removal by MNPs at different dosage of 40, 80, 120, 160, 200, and 240 mg. They indicated that the removal efficiency of Co (II) from the solution increased as the dosage of MNPs rose, which is due to larger number of MNPs sites (Tizro & Baseri, 2017). Besides, Ahmad et al. (2019) investigated the effect of a variable adsorbent dosage (0.005–0.03 g/L) of Fe_3O_4/SiO_2/EDTA on the removal of copper as heavy metals. They found that by increasing the adsorbent dosage from 0.005 to 0.01, the maximum removal (95%) was obtained and then almost kept constant (Ahmad et al., 2019).

Rahmani et al. (2010) studied the arsenic removal through NZVI and observed that increasing Fe^0 concentration boosted the removal efficiency. At 10 min reaction time, pH of 7 and Fe concentration of 1 g/L, all of the arsenic was eliminated, but when the concentration of Fe was 0.1 g/L, only 52.1% was removed (Rahmani et al., 2010). Agarwal and Patel (2015) aimed at removing metallic minerals using NZVI and revealed that by raising the adsorbent dosage from 0.1 to 5 g/L, the removal efficiency increased from 75 to 93% but the adsorption capacity reduced, with a maximum dosage of 0.1 and 15.61 mg/g, respectively. In this experiment, the maximum efficiency was observed at a dosage of 1 g/L (Agarwal & Patel, 2015). Kumar et al. (2017) showed that by increasing the dosage of synthesized nanoparticle (nanoscale zero-valent iron-impregnated cashew nutshell) from 0.5 to 3 g/L, the percentage removal of nickel increased from 50 to nearly 100% by expanding available adsorbent sites due to the high dosage of adsorbents (Kumar et al., 2017). Qu et al. (2017) removed hexavalent chromium as an HM from groundwater using activated carbon fiber supported by nanoscale zero-valent iron. The results showed that by increasing the dosage of nano-adsorbent from 0.13 to 0.67 g/L, the removal efficiency of chromium was enhanced from 68.7 to 100%, when the contact time was 30 min. This study confirmed that nano-adsorbent dosage had a positive effect on the removal efficiency of chromium (Qu et al., 2017). In a similar study, Bagbi et al. (2017) showed that by increasing the dosage of L-cysteine (L-cyst) nanoparticle-stabilized zero-valent iron from 1 to 5 g/L under constant conditions (temperature 25 °C, initial concentration of 50 mg/L and pH 5), the removal efficiency of lead also increased from 64 to 99.9% (Bagbi et al., 2017).

The pH value has a significant effect on the adsorption of heavy metals because it determines the amount of adsorbent surface charge, the amount of ionization and the property of the adsorbing material (Salam et al., 2011). The results of evaluating the effect of the pH on the adsorption process by nano-adsorbents show that at high pH values, electrostatic gravity between the ligand and the metal increases, which ultimately leads to more efficient removal (Venkateswarlu et al., 2019). From another aspect, pH affects the structure and can change the level and degree of ionization (Shirsath et al., 2013). In addition, the pH value can affect the solubility of the metal ion since the protons can be adsorbed or released; the ambient acidity affects the ability of hydrogen ions to compete with metal ions inactive sites on the adsorption surface (Ojedokun & Bello, 2016). Besides, it has been reported that, when the pH is less than zero charges (pH_{zpc}), the positive charge level of NZVI eliminates metal cations and reduces the removal efficiency (Tehrani et al., 2015).

Zeinali et al. (2016) synthesized modified carboxymethyl-β-cyclodextrin with MNPs. In this study, pH was altered from 8 to 11, and it was observed that 81.9% of arsenic was removed at basic pH (10), and with a further increase in pH, the arsenic removal efficiency decreases slightly to 81.22% (Zeinali et al., 2016). Zhou et al. (2017) utilized an efficient magnetic (Fe_3O_4) nanocomposite of polypyrrole–graphene oxide for the adsorption of mercury (II) from aqueous media. In this work, and the pH value was varied from 2 to 10. The results indicated that the performance of synthesized nanocomposite is strongly depended on solution pH so that the adsorption capacity of mercury (II) was enhanced to 300 mg/g as pH increased (Zhou et al., 2017).

Moreover, a similar study by Yamini and Safari (2018) confirmed that increasing the pH range from 5 to 9 had a significant effect on the removal of HMs (copper, cadmium, cobalt, manganese, and nickel) from aqueous solutions, and the basic pH of 9 was chosen as the optimum condition (Yamini & Safari, 2018). Also, Dil et al. (2017) used MNPs of γ-Fe2O3 modified using bis (5-bromosalicylidene) -1,3-propandiamine for removing lead from aqueous solutions at the pH values from 2 to 8. They concluded that the adsorption of lead increased significantly from 65 to 95% with higher pH values from 2 to 6, and then, it decreased (Dil et al., 2017).

Liang et al. (2014) removed heavy metal Zn^{2+} by the NZVI. They found that the highest removal efficiency was observed at an initial pH of 5. The Zn^{2+} adsorption gradually increased with larger pH (Liang et al., 2014). A study by Kim et al. (2013) carried out to remove lead using zeolite-nanoscale zero-valent iron composite showed that the removal efficiency of lead was lowered from 99.9 to 93.5% by increasing the pH from 4 to 6 (Kim et al., 2013). Jia et al. (2018) investigated the efficiency of NZVI embedded in super macroporous cryogels for the removal of hexavalent chromium from aqueous solutions. The pH in this study ranged from 2 to 12. The results demonstrated that by increasing the pH from 2 to 12, the adsorption capacity of chromium decreased from 140 to 90 mg/g (Jia et al., 2018).

In the adsorption process, it is important to investigate the effect of the initial concentrations of HMs. It has been mentioned that at the beginning of the process, the adsorbent capability of the adsorbent is high due to the presence of large active sites while with further increase in initial concentrations of HMs, the adsorbent sites will be saturated by HMs, thereby decreasing the adsorbent capacity [204]. Ahmadi et al. (2017) used maghemite (γ-Fe_2O_3) nanoparticles supported on cross-linked chitosan (γ-Fe_2O_3@CS) as a reliable adsorbent to remove cadmium from contaminated water. In this study, the initial concentration of cadmium metal ranged from 5 to 25 mg/L. The results of the study showed that complete removal of cadmium was achieved at an initial concentration of 5 mg/L under constant conditions (duration 60 min, the adsorbent dose of 1.5 g/L, and the pH of 5 ± 0.2). Then, with increasing the concentration up to 25 mg/L, the removal efficiency decreased from 100 to 71% (Ahmadi et al., 2017). Wang et al. (2016) evaluated the performance of new MNPs of Fe_3O_4@SiO_2-SH for the elimination of mercury from aqueous solutions. The results showed that by rising the initial concentration of mercury from 5 to 100 mg, the maximum adsorption capacity of mercury was enhanced from 25 to 132 mg/g, and removal efficiency of mercury diminished from 99.8 to 26.4% (Wang et al., 2016).

The study by Huang et al. (2015) showed that the zero-valent iron nanoparticles modified with sodium dodecyl sulfate are able to remove chromium (VI) from an aqueous solution. It was revealed that the removal efficiency of chromium (VI) was approximately 100% at the concentration of Cr (VI) below 80 mg/L so that at a low concentration, adsorption sites can effectively remove chromium (VI) (Huang et al., 2015). In another study by Arshadi et al. (2014), the performance, mechanism, kinetics, and thermodynamics of the

synthesized NZVI as an adsorbent have been investigated for lead removal, when the initial concentration of metal ions ranged from 5 to 1000 mg/L. The results showed that with higher initial concentration, the adsorption capacity of the metal also increased (Arshadi et al., 2014). Yu et al. (2020) treated a contaminated water with lead using nano-iron supported with bentonite/graphene oxide (GO-B-nZVI). In this work, the effect of lead concentrations from 100–500 mg/L on the removal of lead was studied, and they concluded that under constant conditions (24 h, temperature 18 °C and pH 5 ± 0.3), the rate of lead ion removal reduced by higher initial concentration (Yu et al., 2020). Based on the previous research, it has confirmed that at low concentrations, sufficient adsorption sites are available for adsorption of the Pb (II) while by increasing Pb (II) concentrations, the availability of adsorption sites is relatively lower than the numbers of heavy metal ions (Meena et al., 2008).

The contact time between the adsorbent and the adsorbate is another parameter that influences the adsorption process. In adsorption systems, contact time plays a critical role regardless of other experimental parameters that affect the adsorption kinetics. In addition, determining the optimal contact time is key for obtaining the highest metal ion removal in adsorption experiments (Ojedokun & Bello, 2016). At the beginning of the process, there is a large number of available active sites so the adsorbent has high efficiency, but with extending the time, adsorbent sites are saturated, and the removal efficiency is reduced consequently (Shirsath et al., 2013). Tizro and Baseri (2016) reported that removal efficiency of copper and lead using MNPs at the contact time varied from 10 to 60 min, and increased by up to 50 min. Fast removal of lead ions using natural zeolite coating magnetite nanoparticles was found at 98% (Tizro & Baseri, 2016). Shahriari et al. (2014) investigated the removal of Cr (+3) using magnetic nanoparticles, with the optimal time of 45 min. It was found that by lengthening the contact time, the removal efficiency was also improved (Shahriari et al., 2014). Huang et al. (2015), who aimed at removing the Cr (+6) metal using zero-valent iron modified nanoparticles, also found that by increasing the contact time to 120 min, the removal efficiency of the metal also was enhanced (Huang et al., 2015). A similar study was carried out by Rahmani et al. (2010) to remove arsenic metal using a synthesized NZVI. It was observed that under constant conditions, the initial concentration of arsenic 10 mg/L and pH 7 and extended contact time enhanced removal efficiency, and the duration of 10 min was chosen as the maximum adsorption time (Rahmani et al., 2010). Shang et al. (2017) developed NZVI particles supported on herb-residue biochar for the adsorption of hexavalent chromium from water. The results showed that by increasing the contact time from 0 to 150 min at the constant condition (metal concentration 4 to 30 mg/L and dosage of 0.2 g/L), the removal efficiency was also increased and 60 min was considered as the equilibrium time (Shang et al., 2017).

6.4 Nano-clays

6.4.1 Physicochemical characteristics

Recently, nano-clays as layered mineral silicates have successfully been applied for the removal of various pollutants from water and wastewater due to unique properties such as non-toxicity, low-cost materials, high cation exchange capacity, high surface area, high surface reactivity, and stability (Elhami & Shafizadeh, 2016; Mahmoudian, 2019). Based on these properties, nano-clays have been extensively employed in a wide range of applications such as polymer nanoparticles, color correction, and wastewater treatment (Patel

et al., 2006). Moreover, clay minerals especially bentonite have been suggested as a new alternative for the adsorption of pollutants because of unique physicochemical properties such as high capacity, great heat resistance, low cost, and recyclability (El Haouti et al., 2019).

Various physicochemical properties of nano-clays (BET, SEM/FESEM, FTIR, and XRD) have been discussed based on Table 7. As can be observed, hydroxyl groups can appear at peak 1629.97, 3626, 3440, 3423.76, and 1639 cm^{-1}. The peaks at 798.04, 1035, 529, and 694.4 cm^{-1} are attributed to bending stretching of SiO; moreover, it should be mentioned that inner and outer surface OH stretching vibration are associated with the peak 3698.96, 3620.6, and 3423.76 cm^{-1}, respectively (Soleimani & Siahpoosh, 2015; Yin et al., 2018).

6.4.2 Performance and the effect of variables

The effects of various parameters (adsorbent dosage, pH, initial concentration of HMs, and contact time) have been investigated on the efficiency of nano-clay in the removal of heavy metals. The results of previous research works confirmed that by raising the adsorbent dosage, the removal efficiency of the system is also increased, which is associated with larger number of available surfaces for adsorption (Gupta et al., 2016). Moreover, it has been mentioned that the adsorption capacity (mg/g) of the system is reduced by increasing the adsorbent dosage (Akpomie & Dawodu, 2015). Previous studies confirmed the aforementioned results. In a study by Soleimani and Siahpoosh (2016), the removal of copper from water using Na^+-cloisite nano-clay has been examined at different dosages of nano-clay from 1 to 10 g/L. According to the results, by increasing the nano-adsorbent dosage, the adsorption of metal ions was enhanced (Soleimani & Siahpoosh, 2015). The results of Sharififard et al. (2018) showed that the removal efficiency of cadmium as an HM from the wastewater using nano-clay/TiO_2 composite was improved by increasing the adsorbent dosage (Sharififard et al., 2018).

Several studies have investigated the effect of the initial pH of the aqueous solutions on the adsorption efficiency of HMs. The results showed that pH affects the binding sites and the interlayer between the adsorbent, the metal ion, and the degree of ionization of the active groups on the adsorbent surfaces (Kumar et al., 2017). In general, they have shown that in lower pH values (acidic pH), the percentage of metal ion removal is low, but the adsorption performance of HMs will be improved by raising the pH (Ojedokun & Bello, 2016). On the other hand, in lower pH, there are many H^+ ion on the surface of adsorbents that lead to the build-up of positive levels on the sites. Therefore, due to the strong competition between metal ions and H^+, the removal efficiency of the system will be reduced (Boparai et al., 2013). In a study by Elhami and Shafizadeh (2016) mercury (ii) adsorption by modified nano-clay was investigated at a pH of 2–6. The results demonstrated that the removal of mercury was boosted as the pH increased from 2 to 4 (Elhami & Shafizadeh, 2016). Mojoudi et al. (2019) used activated carbon/nano-clay/thiolated graphene oxide NCs adsorbent to remove lead, and they concluded that the maximum removal of lead (about 98%) occurred at pH 5 but with increasing pH to 7, the adsorption efficiency decreased (Mojoudi et al., 2019).

Researchers studied the effect of initial concentration on the adsorption process, and it has been concluded that the initial concentration of metal is an important driving force for overcoming all resisting metal mass transmissions between the aqueous phase and the solid phase (Shaibu et al., 2014). It is also noted that the removal efficiency of the system

Table 7 The characteristics of nano-clay

Nanoclay	BET (m^2/g)	SEM/FESEM	FTIR	XRD	References
Chitosan-nanoclay	19.01	–	C–O–C stretching: 1.087 cm^{-1}, amide group band of chitosan: 1.628– 1.650 cm^{-1}	Successive intercalation of chitosan	Malayoglu (2018)
Nano-Illite/Smectite Clay	39.46	–	Inner surface OH stretching vibration: 3698.96 and 3620.6 cm^{-1}, outer surface OH stretching vibration: 3423.76 cm^{-1}, OH bending of water: 1629.97 cm^{-1}, Si–O–Si stretching vibration: 1031.99 and 470.19 cm^{-1}, Al–OH bending vibrations: 912.4 cm^{-1}, Si–O stretching vibration: 798.04 and 694.4 cm^{-1}	Mainly composed of quartz, mixed-layer illite/smectite, illite, and kaolinite	Yin et al. (2018)
Ghezeljeh nanoclay	–	The distance between the plates is Nano	OH stretching region: 3626 cm^{-1}, Si–O in-plane stretching: 1035 cm^{-1}, Si–O bending vibrations: 529 cm^{-1}, bending vibrations for the hydroxyl groups of water molecules: 3440 and 1639 cm^{-1}	Nano-clay was composed of montmorillonite minerals	Soleimani and Siahpoosh (2015)
Pillared ilerite nanoclay	45	A thin rectangular plate shape of Nailerite crystallites	O–H stretching vibration: 3800–3100 cm^{-1}, silanol groups: 3500 cm^{-1}, water molecules bending vibrations (δ HOH): 1640 cm^{-1}, symmetric stretching vibrational modes of Si–O–Si linkages: 450 and 550 cm^{-1}	Amorphous phase as a pillar formed between the interlayers	Salam et al. (2021)

is reduced by higher initial concentrations because of the larger number of metal ions than active adsorption sites at higher initial concentrations (Diva et al., 2017). In removing lead metal from aqueous solutions using nano-illite/smectite clay, Yin et al. (2018) observed that the efficiency of the process decreased slightly (from 99.45 to 98.90%) by increasing the initial concentration from 0.25 to 5 mg/L (Yin et al., 2018).

Contact time is another factor affecting adsorption processes so that the removal of HMs is initially quick but decreases with longer contact time, and this trend can be associated with a large number of active sites in adsorbents. Conversely, with the increase and saturation of these sites, the efficiency of the adsorption process is reduced (Dehghani et al., 2015). Almasri et al. (2018) used hydroxy iron-modified montmorillonite nanoclay as an adsorbent to remove arsenite (As (III)). The contact time varied up to 120 min, and the results showed under constant conditions (initial concentration of 1 mg/L, mixing speed of 350 rpm, pH equal of 3 and adsorbent dose of 80 mg/L) with longer contact time, removal efficiency also increased to about 90% (Almasri et al., 2018).

6.5 Carbon nanotubes (CNTs)

6.5.1 Physicochemical characteristics

Carbon nanotubes (CNTs) were discovered in 1991 by Iijima, and it has been proven that the main source of CNTs is carbon, which attracted the attention of many researchers due to unique properties such as electrical properties, high electron mobility, high electrical conductivity, remarkable chemical stability, high porosity, hollow structure, possible to perform controlled modification/activation of their surfaces, and specific surface areas (Mousavi & Janjani, 2018; Mubarak et al., 2016; Obayomi et al., 2020; Šolić et al., 2021). Carbon nanotubes have high levels of layered and hollow structures with high levels that enhance adsorption efficiency for different types of contaminants especially metal ions (Ruparelia et al., 2008). Besides, researchers have found that nanotubes provide a faster flow rate because of their smooth inner surface, which saves energy (Gangadhar et al., 2012). These classes of NPs are a new type of adsorbent that has attracted special attention for the removal of various pollutants such as herbicides and chlorobenzenes, as well as lead and cadmium ions. Additionally, it has been demonstrated that CNTs have excellent ability to remove bacterial pathogens and other biological impurities from contaminated water. The quantum application is a major candidate technique to improve the efficiency of nano-adsorbents of CNTs, which creates functional groups on the surface of nanoparticles. Generally, modification of CNTs can be applied using agents like acid and molecules such as amide, esters and amines (Dehaghi, 2014; Kapinder 2017). Carbon nanotubes can also be categorized into single-wall carbon nanotubes (SWNTs) and multi-walled carbon nanotubes (MWCNTs) based on the number of layers so that they can be applied for the removal of organic and inorganic compounds such as paint, benzene and heavy metals (Hossini et al., 2015) (Hossini et al., 2015). Graphene oxide (GO) is a nanocarbon material with two-dimensional structure that can be produced by chemical oxidation of graphite (Sheet et al., 2014). This type of nano-carbon material has achieved tremendous attention due to its outstanding characteristics such as unique optical, electrical, and mechanical properties, the presence of two-dimensional base levels, simple synthesis process, and a high specific surface area of more than 2630 m^2/g (Guo et al., 2018; Kapinder 2017). Also, GO contains several functional groups such as epoxy (C–O–C), hydroxyl (OH), and carboxylic group (COOH) (Abdi et al., 2018). Studies on the surface topography of the adsorbent can

provide valuable information about the interaction between the adsorbent particles and molecules (Lobo et al., 2010). Physicochemical characteristics of CNTs (nanoparticles size, functional groups, crystalline structure, specific surface area, and chemical structure) can be determined by various techniques such as SEM, transmission electron microscopy (TEM), XRD, BET, and FT-IR (Abd El-Latif et al., 2013; Dehghani et al., 2015; Khodadadi et al., 2015; Madivoli et al., 2016). Table 8 demonstrates characteristics of various CNTs for HMs removal. It has been found that CNTs had a low S_{BET} (76.2 m^2/g) using 8-hydroxyquinoline- MWCNTs (Kosa et al., 2012) and a wide surface area of 700 m^2/g associated with SWCNTs (Dehghani et al., 2015). Generally, based on the results of surface morphology using SEM, it was found that diameter size of CNTs varied between 10 to 70 nm (Bhanjana et al., 2017; Kosa et al., 2012; Salam et al., 2020; Yaghmaeian et al., 2015). FTIR spectrum demonstrated several functional groups; O–H stretching vibration appeared at 3425, 3433, and 3438 cm^{-1}. The peak at 1734 and 1730 cm^{-1} represented the C=O stretching vibration, C-O stretching vibration detected at 1085 and 1051 cm^{-1}, the peaks at 1517 and 1700 cm^{-1} are related to N–H stretching vibration and carboxylic acids, respectively. Moreover, C=N band and N–H stretching vibration are observed at peak 1630 and 1517 cm^{-1} (Bhanjana et al., 2017; Kosa et al., 2012; Mobasherpour et al., 2014; Salam et al., 2020; Yaghmaeian et al., 2015; Zhan et al., 2019).

6.5.2 Performance and the effect of variables

Adsorbent dosage is a key parameter in determining adsorption capacity (Pirbazari et al., 2014). Many studies have shown that by increasing the adsorbent dosage, the amount of the adsorbed material increases, but the adsorption capacity (mg/g) is reduced. It is easily understood that the number of available adsorption sites becomes larger by higher adsorbent dosage, which ultimately increases the removal efficiency (Aljeboree et al., 2017). In a study conducted by Yaghmaeian et al. (2015) to remove mercury from aqueous solutions using MWCNTs, the effect of adsorbent dosage (0.2 to 1 g/L) on the process has been investigated. The results showed that the adsorption of mercury increased when the dosage of CNTs rose from 0.2 to 0.5 (Yaghmaeian et al., 2015). Dehghani et al. (2015) investigated the efficiency of SWCNTs and MWCNTs for the elimination of chromium at an initial concentration of 0.2 mg/L and pH of 2.5. They concluded that the efficiency of chromium removal using SWCNTs and MWCNTs improved by increasing the adsorbent dosage (Dehghani et al., 2015).

Researchers considered the pH value as an important and effective parameter in the adsorption process because the value of pH can determine the surface properties of adsorbents like the active groups (Yaghmaeian et al., 2015). It is well documented that at the pH levels above the zero point of charge (pH > pHpzc), the adsorbent load level is negative; thus, metals are adsorbed on the adsorbent surface (Dehaghi, 2014). In a study, which was carried out by Kosa et al. (2012) for the removal of the Cu (II), Pb (II), Cd (II), Zn (II) metals from nano-sized carbon nanotubes, pH changed from 3 to 9, and it was observed that by increasing the pH, the removal rate of metals also enhanced (Kosa et al., 2012). Dehghani et al. (2015) investigated the removal efficiency of chromium using SWCNTs and MWCNTs. In this study, the pH varied from 2.5 to 9, and the results confirmed maximum removal of Cr (VI) (approximately more than 75 and 95% by both SWCNTs and MWCNTs, respectively) obtained at lower pH (Dehghani et al., 2015). Zhan et al. (2019) applied amino-functionalized CNT-graphene hybrid aerogels as an efficient adsorbent for removing HMs (copper and lead) from the environmental solution. The pH was studied

Table 8 Characteristics of CNTs

CNTs	BET (m^2/g)	SEM/FESEM	FTIR	XRD	References
SWCNTs	700	Porous morphological structure	Cylinder like carbon structure: 1580 cm^{-1}, vibrations in the planes of the graphene sheets: 1500–1600 cm^{-1}	The graphene structure of carbon nanotubes was confirmed	Dehghani et al. (2015)
8-hydroxyquinoline-MWCNTs	76.2	Rope-like, curved, and highly tangled tubes with diameters between 20 and 40 nm	–OH absorption band: 3433 cm^{-1}, C=O stretching vibrations: 1730 cm^{-1}	–	Kosa et al. (2012)
MWCNTs-5,7-dinitro-8-quinolinol	–	MWCNTs were rope-like, curved, and entangle around each other with inner diameters of 18–25 nm	O–H stretching vibration: 3438 cm^{-1}, asymmetric and symmetric stretching vibrations of the NO_2 group: 1583 and 1548 cm^{-1}	–	Salam et al. (2020)
graphene/polydopamine modified MWCNT	117.3	Hybrid aerogels with different mass ratios	C-O stretching vibration in the alkoxy groups: 1085 cm^{-1}, O–H deformation vibrations: 1406 cm^{-1}, C=O stretching vibration in the carbonyl and carboxyl groups: 1734 cm^{-1}, C=N band: 1630 cm^{-1}, N–H stretching vibration: 1517 cm^{-1}	The cellular structure of the hybrid aerogel consists of few-layer graphene nanosheets	Zhan et al. (2019)
MWCNTs	–	The width of synthesized nanotubes is in the range of 60–70 nm	–	Synthesized NPs has all characteristic reflections of CNTs	Bhanjana et al. (2017)

Table 8 (continued)

CNTs	BET (m^2/g)	SEM/FESEM	FTIR	XRD	References
MWCNTs	270	Diameters of MWCNTs was 10–30 nm	Free hydroxyl groups: 3755 cm^{-1}, O–H stretch from carboxyl groups: 3443 cm^{-1}, carbonyl groups: 1633 cm^{-1}, C–O: 1051 cm^{-1}, carboxylic acids, and phenolic groups (O–H): 1459 cm^{-1}, CH_2: 2923 cm^{-1}	–	Yaghmaeian et al. (2015)
MWCNT	102	–	Hydroxyl groups or carbonyl groups: 1580 cm^{-1}, carboxylic acids: 1700 cm^{-1}, hydroxyl groups: 3425 cm^{-1}	–	Mobasherpour et al. (2014)

from 2 to 7, and the results revealed that by increasing the pH from 2 to 5, the adsorption capacity of HMs was enhanced significantly and then decreased (Zhan et al., 2019). In addition, the results of a study by Bhanjana et al. (2017) showed that the best condition for the removal efficiency of cadmium was obtained at higher pH (Bhanjana et al., 2017).

Availability of metal ions in the contaminated environment depends on the sources of contamination with the different concentrations; therefore, it is essential to study the various effects of the initial concentration of HMs on the adsorption process (Kosa et al., 2012). The results of evaluating the effect of the initial concentration of HMs on the adsorption process indicated that by increasing the initial concentration of HMs, the transfer of pollutants to the adsorbent sites has been prevented, which leads to the saturation of active adsorbent sites, thereby reducing adsorbent efficiency in the removal of HMs (Salam et al., 2020). Mobasherpour et al. (2014) reported the adsorption of copper at different conditions (initial concentrations of 10–30 mg/L, pH = 7, 700 rpm, contact time of 120 min, and 0.8 g/L from t-MWCNT) and found that adsorption of copper ion was improved by increasing initial metal concentration (Mobasherpour et al., 2014). Rashid et al. (2019) synthesized sulfonated polyethersulfone-reinforced MWCNTs composite to remove lead from wastewater. They indicated that by increasing the initial concentration of lead from 10 to 100 mg/L, the adsorption capacity of lead increased from 7 mg/g to 48 mg/g (Rashid et al., 2019).

Investigating the effect of contact time as a decisive factor is essential to evaluate the equilibrium and the kinetics of the adsorption process (Anbia & Amirmahmoodi, 2016). At the beginning of the process, more active sites are available for the adsorption of HMs. Therefore, the adsorbent efficiency is high but with further increase in the contact time, the adsorbent sites are saturated from the HMs, so the efficiency of the system diminished (Shirsath et al., 2013). Furthermore, contact time can be used to describe the interaction between the adsorbate and adsorbent as well as adsorbent efficiency, so that the faster the removal means the better the adsorbent (Kosa et al., 2012).

Dehghani et al. (2015) have used CNTs to remove chromium, and they found that the removal efficiency of chromium was enhanced as contact time increased (equilibrium time was obtained after 60 min). In this experiment, the maximum adsorption capacity using SWCNT and MWCNT was 2.35 mg/g and 1.26 mg/g, respectively. The main reason for decreasing slightly of efficiency with an increasing time can be related to the abundant number of active sites present on the adsorbents, whereas, with the gradual increased occupancy of these sites, the adsorption process becomes less efficient (Dehghani et al., 2015). In a similar study, Al-Khaldi et al. (2015) used carbon nanotubes to remove cadmium, which showed that the removal efficiency also increased with extending the contact time (Al-Khaldi et al., 2015).

7 Comparison study

The efficiency of many inorganic nano-adsorbents for the removal of the most challenging environmental HMs such as Pb (II), As (III), Cd (II), Cr (VI), Cu (II), Ni (II) was compared based on major operational factors (pH, initial concentration of HMs, and contact time) (Table 9). It should be considered that for better comparing the adsorption efficiency of various NPs, it is useful to apply partition coefficient (PC) or sorption distribution coefficient (DC) (mg/g μM), which can be calculated as the ratio of adsorption capacity to a final concentration of adsorbed HMs or is the ratio of sorbed metal concentration (expressed

Table 9 Comparison of HMs removal efficiency using various inorganic nano-adsorbents

NPs	Adsorbent	Adsorbate	Initial C_0 (μM)	Maximum capacity (mg/g)	Final C_0 (μM)	pH	Time (min)	Removal (%)	PC (mg/g/μM)	References
NMOs	TiO_2	Hg (I) Hg (II)	50 40	114.9 90.9	1.25 0.56	9 7	75 45	97.5 98.6	91.92 162.321	Afshar et al., (2017)
	ZnO	Pb^{2+}	96.52	26.109	0.024	5	180	99.99	1087.88	Venkatesham et al. (2013)
	Guar gum–ZnO	Cr(VI)	25	55.56	1.25	7	50	96	44.48	Ali et al. (2017)
	MgO	Pb^{2+} Cr^{6+}	48.26 192.32	21.78 16.44	9.02 10	9	280	81.25 94.78	2.41 1.64	Dargahi et al. (2015)
NCs	Fe@MgO magnetic	Pb(II)	723.93	1476.4	9.41	6	30	98.7	156.89	Ge et al. (2018)
	$FeNi_3$@SiO_2 magnetic	Pb(II)	4.82	588.23	0.57	6	20	88	1031.98	Farooghi et al. (2018)
	Fe_3O_4/Talc	Cu(II) Ni(II) Pb(II)	1573.66 1567.47 1303.08	21.05 33.33 74.62	439.05 778.62 112.69	actual	2	72.1 50.23 91.35	0.047 0.042 0.66	Kalantari et al. (2014)
	Silver-yttrium oxide	Cu(II) Cr(VI)	1573.66 1923.22	853 878	966.22 1184.70	6	720	38.6 38.4	0.88 0.74	Pradhan et al. (2017)
MNPs	γ-Fe2O3 modified by bis(5-bromosalicylidene)-1,3-propandiamine	Pb^{2+}	72.39	163.57	0.11	4	4	99.77	1487	Dil et al. (2017)
	Graphene oxide-Fe_3O_4	Pb(II)	471.42	777.28	19.93	6	10	95.77	39	Guo et al. (2018)
	amine-functionalized Fe_3O_4	Cu(II)	157.36	25.77	3.14	6	5	98	8.20	Hao et al. (2010)
	Fe_3O_4@SiO_2-SH	Hg(II)	99.70	133.3	0.029	6	–	99.97	4596.55	Wang et al. (2016)

Table 9 (continued)

NPs	Adsorbent	Adsorbate	Initial C_0 (μM)	Maximum capacity (mg/g)	Final C_0 (μM)	pH	Time (min)	Removal (%)	PC (mg/g/μM)	References
NZVI	L-Cysteine (L-cyst) stabilized NZVI	Pb^{2+}	241.31	36.8	0.24	6	25	99.9	153.33	Bagbi et al. (2017)
	NZVI -impregnated cashew nutshell	Ni (II)	425.94	70.05	0.037	5	30	99.99	1893.24	Kumar et al. (2017)
	NZVI—sodium dodecyl sulfate	Cr (VI)	5769.67	264.55	62.36	3	120	98.919	4.24	Huang et al. (2015)
	Zeolite– NZVI composite	Pb(II)	482.62	806	19.29	-	140	96	41.78	, Kim et al. (2013)
Nano clays	Nano-clay/TiO2 composite	Cd (II)	266.877	16.20	26.687	6	–	90	0.607	Sharififard et al. (2018)
	Activated carbon/ nanoclay/ thiolated graphene oxide	Pb(II)	241.312	208	4.826	5	60	˃98	43.09	Mojoudi et al. (2019)
	Nano-illite/smectite clay	Pb(II)	1.206	0.256	0.006	4	20	99.4	42.73	Yin et al. (2018)
	Hydroxy iron-modified montmorillonite (HyFe-MMT) nanoclay	As(III)	13.34	3.854	1.327	3	120	90	2.904	Almasri et al. (2018)
CNTs	MWCNT	Cd^{2+}	889.6	181.8	43.59	8	–	95.1	4.17	Bhanjana et al. (2017)
	CNT	Cd^{2+}	8.89	0.65	6.49	7	–	27	0.1001	Al-Khaldi et al. (2015)
	SWCNT and MWCNT	Cr (VI)	3.84	SWCNT = 2.35 MWCNT = 1.26	1.152 0.384	3	60	70 whit SWCNT 90 whit WCNT	2.03 3.28	Dehghani et al. (2015)

in mg metal/kg sorbing material) to the dissolved metal concentration (expressed in mg metal/L of solution) (Allison & Allison, 2005; Tran et al., 2016; Vikrant et al., 2019). The PC can be deemed as one of the major environment parameter and is a measure of solute sorption or affinity to matrix surfaces (Elbana et al., 2018). This parameter has linear relationship with ability of the sorbent in adsorption process so that at the higher value of the distribution coefficient, the greater ability of the sorbent to retain the species of interest can be observed (Engates & Shipley, 2011). Therefore, it is essential to calculate the true performance of each NP using PC value; in this regard, we altered the value of the initial and final concentration of HMs (mg/L) to μM to obtain the PC value. Based on Table 9, it can be understood that for most NPs, higher PC value was attained at a low initial concentration of HMs; nonetheless, some NPs do not confirm to the above aforementioned finding (Bhanjana et al., 2017; Guo et al., 2018; Mojoudi et al., 2019; Pradhan et al., 2017; Venkatesham et al., 2013). It can be found that among the NMOs, the highest partition coefficient was related to ZnO (1087.88 mg/g/μM). ZnO as an alternative inorganic NPs can be widely employed for HMs removal (Venkatesham et al., 2013). According to the unique properties of the MNPs, it was observed that Fe_3O_4@SiO_2-SH with a PC of 4596.55 mg/g/μM had the best efficiency compared to the other MNPs (Wang et al., 2016). It should be noted that NZVI -impregnated cashew nutshell with PC of 1893.24 55 mg/g/μM was chosen as the most effective adsorbent among all NZVIs (Kumar et al., 2017). The results of a study by Farooghi et al. (2018) demonstrated that the $FeNi_3$@SiO_2 with a high PC of 1031.98 mg/g/μM has an excellent capability for the removal of HMs (especially lead) from aqueous solutions as compared with other nanocomposites (Farooghi et al., 2018). Among the nano-clays, activated carbon/nano-clay/ thiolated graphene oxide and nano-illite/smectite clay demonstrated the best adsorption condition with the PC of 43.09 and 42.73 mg/g/μM, respectively (Mojoudi et al., 2019; Yin et al., 2018). Also, MWCNT as carbon nanotube (4.17 mg/g/μM) had the best efficiency for the adsorption of HMs (Bhanjana et al., 2017). The results of Table 9 conclusively depicted that inorganic nano-adsorbents had an excellent efficiency for the removal of HMs, and therefore, they can be deemed as effective, suitable, and reliable candidates for the treatment of water and wastewater containing many pollutants specially HMs.

8 Nano-adsorption Kinetics and isotherms

Kinetic adsorption is the study of the adsorption process to understand the factors affecting the adsorption process. The kinetics of adsorption involves careful monitoring of experimental conditions that are based on the adsorption rate and the equilibrium over a reasonable time (Li et al., 2012). To examine the behavior of NPs for HMs removal, various kinetic models such as pseudo-first-order (PFO) (Yaghmaeian et al., 2015), pseudo-second-order (PSO) (Foo & Hameed, 2012), intraparticle diffusion (IPD) (Nethaji et al., 2013), and Elovich (El-Sadaawy & Abdelwahab, 2014) have been studied. Among them, PFO and PSO have been widely used for the adsorption of HMs using several inorganic NPs in previous works. Furthermore, equations and major application of the aforementioned kinetic models are summarized in Table 10.

An adsorption isotherm is an important tool for evaluating the adsorbent distribution on solid/liquid boundaries and can be used to estimate the adsorption capacity (Nanta et al., 2018). Previous research works have confirmed that the interaction between adsorbate and adsorbent can be obtained by adsorption isotherms models (Altıntıg et al., 2017). Exerting

Table 10 Kinetic models and equations

Kinetic Models	Equations models	Constant parameters	Application	References
PFO	$\frac{d_{qt}}{d_t} = kl(q_e - q_t)$ $\log(q_e - q_t) = \log q_e - \frac{kl}{2.303}t$	q_t is the amount of adsorbed at any time (mg/g) K_1 is the adsorption rate constant K_2 is the adsorption rate constant	To estimate the initial stage of the adsorption mechanism	Reddy et al. (2014), Yaghmaeian et al. (2015)
PSO	$\frac{1}{q_e - q_t} = \frac{1}{q_e} + k_{2*}t$	k_i is the intraparticle diffusion rate constant	Suggests chemisorption process	Foo and Hameed (2012), Prajapati and Mondal (2020)
IPD	$q_t = k_i * t^{\frac{1}{2}} + c_i$	α is the initial sorption rate (mg/(g min))	To detect the pathway involved in the adsorption system	Nethaji et al. (2013), Reddy et al. (2014)
Elovich	$q_t = \frac{1}{\beta}\ln(\alpha\beta) + \frac{1}{\beta}\ln t$	β is the de-sorption constant (g/mg)	To examine chemisorption	El-Sadaawy and Abdelwahab (2014), Prajapati and Mondal (2020)

isotherms (commonly named equilibrium relationships) in the adsorption processes can be useful for several purposes such as: (1) to represent the physicochemical characteristics (especially surface properties) and adsorbents capacities; (2) to optimize the adsorption process pathways; and (3) to develop an efficient design of the adsorption systems (El-Khaiary, 2008). Up to now, several isotherm models by Longmuir (Fard et al., 2018; Nanta et al., 2018), Freundlich (Bao & Zhang, 2012; Kaveeshwar et al., 2018), Temkin (Foo & Hameed, 2012), Sips (Pirbazari et al., 2014), and Dubinin-Radushkevich (D-R) (Chaudhry et al., 2017) have been applied to describe equilibrium relations. Notably, among the aforementioned isotherm models, two famous isotherm models of Freundlich (Freundlich, 1906) and Longmuir isotherm models (Langmuir 1918) were obtained for equilibrium data of inorganic NPs (Bao & Zhang, 2012). Other isotherm models and their main application are listed in Table 11.

Furthermore, as explained above, to better scrutinize the importance of isotherm-kinetic models and adsorption mechanisms, it is necessary to compare several studies. Therefore, in this section, adsorption isotherms and kinetics, experimental data, correlation coefficients, and their constants of various NPs, which were applied for HMs removal, are compared in Table 12. As can be detected, among the suggested isotherm models (Langmuir, Freundlich, and Tempkin), the experimental data for most groups of inorganic nanoadsorbent were best described by the Langmuir isotherm with a regression coefficient (R^2) of greater than 0.93. It thoroughly confirmed that the adsorption is a monolayer (Alswata et al., 2017; Dehghani et al., 2015; Dil et al., 2017; Mobasherpour et al., 2014)*).* Nevertheless, among the studies, there was only one work in which the experimental data of the adsorption process was best fitted with Freundlich isotherms with $R^2 = 0.99$ (Huang et al., 2015). *Moreover, i*t was found that between the two kinetics (PFO and PSO), the pseudo-second-order kinetics is *more frequently used and best fitted for the removal of HMs from aqueous solution by inorganic NPs* because of the R^2 in the range of 0.98 to 0.99. As stated before, it can be observed that HMs adsorption from an aqueous solution is based on the chemisorption process (Foo & Hameed, 2012; Prajapati & Mondal, 2020).

9 Negative effects of nanomaterials

Nanotechnology is a fascinating and promising technology in many areas, because of the novelty of this science, but the risk associated with the use of nanomaterials has not been studied well and it is gradually becoming a public and media concern (Moore, 2006). Based on the data, it has been estimated that about 2000 tons of NPs were produced in 2004 (Taghavi et al., 2013), and it can be expected that the production rate of this type of materials will grow up to 58,000 tons by 2020, so it is critical to determine the hazardous effects of NPs (Taghavi et al., 2013). A growing number of experiments are currently underway to explore the impact of nanoscale particles on human health. The results indicated smaller particles (< 50 nm) are toxic to inhale because they penetrate into the body by type II lung epithelial cells (Yang & Watts, 2005). The toxicity effect of nanoparticles can be associated with (1) average size, (2) element composition, (3) surface area, (4) porosity, (5) surface charge, (6) hydrodynamic diameter, (7) tendency to aggregate, and (8) stability (Dietz & Herth, 2011). Consequently, we can note the adverse effects of nanoparticles on the living and human health as follows: (a) they affect the heart (Chen et al., 2015); (b) they can cross the blood–brain barrier and gather in three separate regions of the respiratory system (nose, throat, the trachea and lung

Table 11 Isotherms models and equations

Isotherms Models	Equations models	Constant parameters	Application	Reference
Langmuir	$q_e = \frac{q_0 * b * c_e}{1 + b * c_e}$ $\frac{c_e}{q_e} = \frac{1}{K_L * q_m} + \frac{c_e}{q_m}$	q_e is the amount of adsorbed at equilibrium (mg/g) C_e is a metal concentration in the aqueous phase (mg/L) b is Langmuir equilibrium constant (L g adsorbent^{-1}) q_0 is maximum monolayer adsorption (mg g adsorbent^{-1}) k_L is the Langmuir constant (L/mg) K_F and n are Freundlich coefficients Temkin constant is $B = RT/b$ and b (J mol^{-1}) is the adsorption heat An (L g^{-1}) is fixed Temkin isotherm R (3314 J mol^{-1} K^{-1}) is a constant global gas in which T (K) is absolute $Q_{D\text{-}R}$ (lg/g) is the theoretical saturation capacity of the adsorbent b is a constant related to the mean free energy of adsorption per mole of the adsorbate ε is a logarithmic function of concentration called Polanyi potential. R and T are gas constant and temperature in Kelvin scale	To express the single-layer adsorption process	Fard et al. (2018), Nanta et al. (2018), You et al. (2016)
Freundlich	$1/nQ = k_f * (c_e)$ $\ln q_e = \ln k_f + \frac{1}{n} \ln c_e$		To suggest the heterogeneous structure of the adsorbent surface	Bao and Zhang (2012), Kaveeshwar et al. (2018), Nasrullah et al. (2018)
Temkin	$q_e = B \ln A * C_e$ $q_e = B \ln A + B \ln C_e$		Assumes the heat of adsorption, effects of indirect interaction between adsorbent molecules has predictive power in a wide range of concentrations	Foo and Hameed (2012), Kaveeshwar et al. (2018), Njoku et al. (2014)
D-R	$\ln Q_e = \ln Q_{D-R} - \beta \varepsilon^2$ $\varepsilon = RT \ln(1 + \frac{1}{C_e})$		Is used for the isotherms analysis with a high degree of regularity	Chaudhry et al. (2017), Dubinin (1960)
Sips	$q_e = \frac{Q_{max} K_s C_e^{1/n}}{(1 + K_s C_e^{1/n})}$		Is an alternative empirical approach with the characteristics of the Freundlich and Langmuir isotherms	Pirbazari et al. (2014)

Table 12 Isotherm and kinetic constants of various nano-adsorbents

NPs	Adsorbate	Isotherm constants						Kinetic constants						References
		Langmuir			Freundlich			PFO			PSO			
		q_m (mg/g)	K_L (l/mg) or b	R^2	K_F	1/*n*	R^2	k_1	q_e	R^2	k_2	q_e	R^2	
MWCNs	Cu (II)	12.34	0.19	0.99	3.72	0.32	0.99	0.092	7.161	0.948	0.117	18.868	0.99	Mobasherpour et al. (2014)
SWCNTs	Cr (VI)	2.35	0.424	0.99	0.279	0.23	0.82	0.003	0.203	0.81	1.555	0.193	0.99	Dehghani et al. (2015)
MWCNs		1.26	0.789	0.98	0.623	0.16	0.77	0.007	0.198	0.98	0.289	0.188	0.99	
TiO_2	Pb^{2+}	7.41	0.35	0.97	2.73	0.29	0.82	0.01	3.27	0.66	12.41	5.78	0.98	Poursani et al. (2016)
NZVI	Cr (VI)	264.55	0.1432	0.93	45.82	0.043	0.99	0.01	98.39	0.90	0.3125	98.3	0.99	Huang et al. (2015)
Zeolite/Zinc Oxide NCs	Pb (II) As (V)	47.6	0.13	0.99	2.3	0.66	0.97	0.06	18.7	0.99	0.004	27.7	0.99	Alswata et al. (2017)
Silver-yttrium oxide NCs	Cu (II)	0.003	22.3	0.99	2.5	0.68	0.98	0.043	16.4	0.955	0.003	22.3	0.99	Pradhan et al. (2017)
Carboxymethyl-β-cyclodextrin modified MNPs	As (III)	12.330	0.171	0.98	1.57	1.52	0.97	0.077	0.834	0.96	0.256	6.917	0.99	Zeinali et al. (2016)
Modified MNPs	Pb^{2+}	163.57	25.18	0.99	8.85	0.49	0.91	2.74	3.69	0.735	4.15	144.70	0.99	Dil et al. (2017)

alveoli) and can penetrate into the sensory nerves (Baranowska-Wójcik et al., 2020); finally (c) they can penetrate into the skin and cause toxic effects such as skin cytotoxicity during accumulation of NPs upon long exposure (Tsuji et al., 2006). Moreover, nanomaterials can be directly deposited into the environment (water surface, land, soil) (Ray et al., 2009). Based on the above explanation, new studies should be considered to evaluate the toxicity and the main adverse effect of NPs on human health and the ecosystem.

10 Conclusion and future developments

Over the past few decades, several techniques have made great progress for water/wastewater purification containing HMs. Among them, adsorption techniques are a simple method in removing pollutants, but the application of this method has been restricted because of resistance to the massive mass transport. To overcome their drawbacks, recently, inorganic nano-adsorbents have been utilized as next-generation adsorbents due to noteworthy features (larger surface areas, higher selectivity, stability, and amendable size and shape) in removing HMs. In this regard, we have completely highlighted the efficiency of inorganic nano-adsorbents for HMs decontamination from environmental solution by evaluating various adsorption parameters (initial concentration of HMs, nano-adsorbents dosage, contact time, and pH). Besides, the comparison of several isotherm and kinetic models has been taken into account. Generally, the results confirmed that this type of nano-adsorbents had a high removal efficiency for HMs (approximately more than 90%). Furthermore, this review revealed that despite extensive application, nanomaterials often have toxic effects on the environment, human beings, and the ecosystem, making it essential to evaluate the toxicity risk. Overall, this comprehensive review paves the way for deeper understanding and application of inorganic nano-adsorbents that would be invaluable for HMs removal.

Although nanoparticles have been shown outstanding properties for the environmental remediation, further researches is needed in the future for completing their limitations. So, herein we have recommended some points that will be helpful for future of researchers as follow as:

- The study on the human and ecological risks associated with nanoparticles, and the release of toxic elements into environment.
- Further interdisciplinary studies and scaling-up strategies would favor the application of these in large scale as an alternative approach.
- The study on the NPs economic.
- The study on the integrating methods (nanoparticles and the other type of treatment methods)

Acknowledgements The authors of this article are well aware of the need to thank Kermanshah University of Medical Sciences.

Declaration

Conflict of interest The authors have no conflicts of interest to declare.

References

Abd El-Latif, M. M., Ibrahim, A. M., Showman, M. S., & Hamide, R. R. A. (2013). Alumina/iron oxide nano composite for cadmium ions removal from aqueous solutions. *Journal of Nonferrous Metallurgy, 2*(2), 47.

Abdi, G., Alizadeh, A., Zinadini, S., & Moradi, G. (2018). Removal of dye and heavy metal ion using a novel synthetic polyethersulfone nanofiltration membrane modified by magnetic graphene oxide/metformin hybrid. *Journal of Membrane Science, 552*, 326–335.

Adeel, S., Kiran, S., Habib, N., Hassan, A., Kamal, S., Qayyum, M. A., & Tariq, K. (2020). Sustainable ultrasonic dyeing of wool using coconut coir extract. *Textile Research Journal, 90*, 744–756.

Adeleye, A. S., Conway, J. R., Garner, K., Huang, Y., Su, Y., & Keller, A. A. (2016). Engineered nanomaterials for water treatment and remediation: Costs, benefits, and applicability. *Chemical Engineering Journal, 286*, 640–662.

Adeli, M., Yamini, Y., & Faraji, M. (2017). Removal of copper, nickel and zinc by sodium dodecyl sulphate coated magnetite nanoparticles from water and wastewater samples. *Arabian Journal of Chemistry, 10*, S514–S521.

Afshar, E., Mohammadi, M. H., Dashti, K. H. (2017). Removal of Hg (I) and Hg (II) ions from aqueous solutions, using TiO_2 nanoparticles.

Agarwal, M., & Patel, D. (2015). Modified zero valent iron (ZVI) nanoparticles for removal of manganese from water. *International Journal of Environmental Research, 9*, 1055–1068.

Agrafioti, E., Kalderis, D., & Diamadopoulos, E. (2014). Arsenic and chromium removal from water using biochars derived from rice husk, organic solid wastes and sewage sludge. *Journal of Environmental Management, 133*, 309–314.

Ahmad, I., Siddiqui, W. A., & Ahmad, T. (2019). Synthesis and characterization of molecularly imprinted magnetite nanomaterials as a novel adsorbent for the removal of heavy metals from aqueous solution. *Journal of Materials Research and Technology, 8*, 4239–4252.

Ahmadi, M., Niari, M. H., & Kakavandi, B. (2017). Development of maghemite nanoparticles supported on cross-linked chitosan (γ-Fe_2O_3@CS) as a recoverable mesoporous magnetic composite for effective heavy metals removal. *Journal of Molecular Liquids, 248*, 184–196.

Akbari, A., & Mohamadzadeh, F. (2012). New method of synthesis of stable zero valent iron nanoparticles (nZVI) by chelating agent diethylene triamine penta acetic acid (DTPA) and removal of radioactive uranium from ground water by using iron nanoparticle. *Journal of Nanostructures, 2*, 175–181.

Akbarzadeh, M. J., Hashemian, S., & Mokhtarian, N. (2020). Study of Pb (II) removal ZIF@ $NiTiO_3$ nanocomposite from aqueous solutions. *Journal of Environmental Chemical Engineering, 8*, 103703.

Akpomie, K., & Dawodu, F. (2015). Potential of a low-cost bentonite for heavy metal abstraction from binary component system. *Beni-Suef Univ J Basic Appl Sci, 4*(1), 1–3.

Al-Khaldi, F. A., Abu-Sharkh, B., Abulkibash, A. M., & Atieh, M. A. (2015). Cadmium removal by activated carbon, carbon nanotubes, carbon nanofibers, and carbon fly ash: A comparative study. *Desalination and Water Treatment, 53*, 1417–1429.

Al-Qahtani, K. M. (2016). Water purification using different waste fruit cortexes for the removal of heavy metals. *Journal of Taibah University for Science, 10*, 700–708.

Aldwayyan, A., Al-Jekhedab, F., Al-Noaimi, M., Hammouti, B., Hadda, T., Suleiman, M., & Warad, I. (2013). Synthesis and characterization of CdO nanoparticles starting from organometalic dmphen-CdI2 complex. *International Journal of Electrochemical Science, 8*, e10514.

Ali, I. (2012). New generation adsorbents for water treatment. *Chemical Reviews, 112*, 5073–5091.

Ali, I., Asim, M., & Khan, T. (2017). Removal of chromium (VI) from aqueous solution using guar gum–nano zinc oxide biocomposites adsorbent. *Arabian Journal of Chemistry, 10*, 2388–2398.

Ali, S., Shah, I. A., Ahmad, A., Nawab, J., & Huang, H. (2019). Ar/O_2 plasma treatment of carbon nanotube membranes for enhanced removal of zinc from water and wastewater: A dynamic sorption-filtration process. *Science of the Total Environment, 655*, 1270–1278.

Aljeboree, A. M., Alshirifi, A. N., & Alkaim, A. F. (2017). Kinetics and equilibrium study for the adsorption of textile dyes on coconut shell activated carbon. *Arabian Journal of Chemistry, 10*, S3381–S3393.

Allison, J. D., & Allison, T. L. (2005). Partition coefficients for metals in surface water, soil, and waste. Rep. EPA/600/R-05, 74.

Almasi, A., Navazeshkhaa, F., & Mousavi, S. A. (2017a). Biosorption of lead from aqueous solution onto Nasturtium officinale: Performance and modeling. *Desalination and Water Treatment, 65*, 443–450.

Almasi, A., Rostamkhani, Z., & Mousavi, S. A. (2017b). Adsorption of Reactive Red 2 using activated carbon prepared from walnut shell: Batch and fixed bed studies. *Desalination and Water Treatment, 79*, 356–367.

Almasri, D. A., Rhadfi, T., Atieh, M. A., McKay, G., & Ahzi, S. (2018). High performance hydroxyiron modified montmorillonite nanoclay adsorbent for arsenite removal. *Chemical Engineering Journal, 335*, 1–12.

Alswata, A. A., Ahmad, M. B., Al-Hada, N. M., Kamari, H. M., Hussein, M. Z. B., & Ibrahim, N. A. (2017). Preparation of zeolite/zinc oxide nanocomposites for toxic metals removal from water. *Results in Physics, 7*, 723–731.

Altıntıg, E., Altundag, H., Tuzen, M., & Sarı, A. (2017). Effective removal of methylene blue from aqueous solutions using magnetic loaded activated carbon as novel adsorbent. *Chemical Engineering Research and Design, 122*, 151–163.

Amadi, E. V., Venkataraman, A., Papadopoulos, C. (2021). Nanoscale self-assembly: Concepts, applications and challenges. *Nanotechnology*. 33, 1361–6528

Amuda, O., Amoo, I., Ipinmoroti, K., & Ajayi, O. (2006). Coagulation/flocculation process in the removal of trace metals present in industrial wastewater. *Journal of Applied Sciences and Environmental Management, 10*, 159–162.

Anbia, M., & Amirmahmoodi, S. (2016). Removal of Hg (II) and Mn (II) from aqueous solution using nanoporous carbon impregnated with surfactants. *Arabian Journal of Chemistry, 9*, S319–S325.

Andrade, L., Aguiar, A., Pires, W., Miranda, G., Teixeira, L., Almeida, G., & Amaral, M. (2017). Nanofiltration and reverse osmosis applied to gold mining effluent treatment and reuse. *Brazilian Journal of Chemical Engineering, 34*, 93–107.

Arshadi, M., Soleymanzadeh, M., Salvacion, J., & SalimiVahid, F. (2014). Nanoscale zero-valent iron (NZVI) supported on sineguelas waste for Pb (II) removal from aqueous solution: Kinetics, thermodynamic and mechanism. *Journal of Colloid and Interface Science, 426*, 241–251.

Asadpour, S., Chamsaz, M., Entezari, M. H., Haron, M. J., & Ghows, N. (2016). On-line preconcentration of ultra-trace thallium (I) in water samples with titanium dioxide nanoparticles and determination by graphite furnace atomic absorption spectrometry. *Arabian Journal of Chemistry, 9*, S1833–S1839.

Azad, H., Mohsennia, M., Cheng, C., & Amini, A. (2021). Facile fabrication of PVB-PVA blend polymer nanocomposite for simultaneous removal of heavy metal ions from aqueous solutions: Kinetic, equilibrium, reusability and adsorption mechanism. *Journal of Environmental Chemical Engineering, 9*, 106214.

Bagbi, Y., Sarswat, A., Tiwari, S., Mohan, D., Pandey, A., & Solanki, P. R. (2017). Synthesis of l-cysteine stabilized zero-valent iron (nZVI) nanoparticles for lead remediation from water. *Environmental Nanotechnology, Monitoring & Management, 7*, 34–45.

Bao, Y., & Zhang, G. (2012). Study of adsorption characteristics of methylene blue onto activated carbon made by Salix psammophila. *Energy Procedia, 16*, 1141–1146.

Baranowska-Wójcik, E., Szwajgier, D., Oleszczuk, P., & Winiarska-Mieczan, A. (2020). Effects of titanium dioxide nanoparticles exposure on human health—A review. *Biological Trace Element Research, 193*, 118–129.

Barkay, T., & Wagner-Döbler, I. (2005). Microbial transformations of mercury: Potentials, challenges, and achievements in controlling mercury toxicity in the environment. *Advances in Applied Microbiology, 57*, 1–52.

Bekhit, F., Farag, S., & Attia, A. M. (2020). Decolorization and degradation of the Azo dye by bacterial cells coated with magnetic iron oxide nanoparticles. *Environmental Nanotechnology, Monitoring & Management, 14*, 100376.

Belkacem, M., Bekhti, S., & Bensadok, K. (2007). Groundwater treatment by reverse osmosis. *Desalination, 206*, 100–106.

Bhakta, J., & Munekage, Y. (2011). Mercury (II) adsorption onto the magnesium oxide impregnated volcanic ash soil derived ceramic from aqueous phase. *International Journal of Environmental Research, 5*, 585–594.

Bhanjana, G., Dilbaghi, N., Kim, K.-H., & Kumar, S. (2017). Carbon nanotubes as sorbent material for removal of cadmium. *Journal of Molecular Liquids, 242*, 966–970.

Bhowmick, S., Chakraborty, S., Mondal, P., Van Renterghem, W., Van den Berghe, S., Roman-Ross, G., Chatterjee, D., & Iglesias, M. (2014). Montmorillonite-supported nanoscale zero-valent iron for removal of arsenic from aqueous solution: Kinetics and mechanism. *Chemical Engineering Journal, 243*, 14–23.

Björkman, L., Lundekvam, B. F., Lægreid, T., Bertelsen, B. I., Morild, I., Lilleng, P., Lind, B., Palm, B., & Vahter, M. (2007). Mercury in human brain, blood, muscle and toenails in relation to exposure: An autopsy study. *Environmental Health, 6*, 1–14.

Boparai, H. K., Joseph, M., & O'Carroll, D. M. (2013). Cadmium (Cd 2+) removal by nano zerovalent iron: Surface analysis, effects of solution chemistry and surface complexation modeling. *Environmental Science and Pollution Research, 20*, 6210–6221.

Bora, A. J., & Dutta, R. K. (2019). Removal of metals (Pb, Cd, Cu, Cr, Ni, and Co) from drinking water by oxidation-coagulation-absorption at optimized pH. *Journal of Water Process Engineering, 31*, 100839.

Brooks, R. M., Bahadory, M., Tovia, F., & Rostami, H. (2010). Removal of lead from contaminated water. *International Journal of Soil, Sediment and Water, 3*, 14.

Byambaa, M., Dolgor, E., Shiomori, K., & Suzuki, Y. (2018). Removal and recovery of heavy metals from industrial wastewater by precipitation and foam separation using lime and casein. *Journal of Environmental Science and Technology, 11*, 1–9.

Chaudhary, S., Kaur, Y., Umar, A., & Chaudhary, G. R. (2016). Ionic liquid and surfactant functionalized ZnO nanoadsorbent for recyclable proficient adsorption of toxic dyes from waste water. *Journal of Molecular Liquids, 224*, 1294–1304.

Chaudhry, S. A., Khan, T. A., & Ali, I. (2016). Adsorptive removal of Pb (II) and Zn (II) from water onto manganese oxide-coated sand: Isotherm, thermodynamic and kinetic studies. *Egyptian Journal of Basic and Applied Sciences, 3*, 287–300.

Chaudhry, S. A., Khan, T. A., & Ali, I. (2017). Zirconium oxide-coated sand based batch and column adsorptive removal of arsenic from water: Isotherm, kinetic and thermodynamic studies. *Egyptian Journal of Petroleum, 26*, 553–563.

Chen, Q., Tang, Z., Li, H., Wu, M., Zhao, Q., & Pan, B. (2020). An electron-scale comparative study on the adsorption of six divalent heavy metal cations on $MnFe_2O_4$@ CAC hybrid: Experimental and DFT investigations. *Chemical Engineering Journal, 381*, 122656.

Chen, Z., Wang, Y., Zhuo, L., Chen, S., Zhao, L., Luan, X., Wang, H., & Jia, G. (2015). Effect of titanium dioxide nanoparticles on the cardiovascular system after oral administration. *Toxicology Letters, 239*, 123–130.

Choudhury, P. R., Mondal, P., & Majumdar, S. (2015). Synthesis of bentonite clay based hydroxyapatite nanocomposites cross-linked by glutaraldehyde and optimization by response surface methodology for lead removal from aqueous solution. *RSC Advances, 5*, 100838–100848.

Chougui, A., Zaiter, K., Belouatek, A., & Asli, B. (2014). Heavy metals and color retention by a synthesized inorganic membrane. *Arabian Journal of Chemistry, 7*, 817–822.

Chunhabundit, R. (2016). Cadmium exposure and potential health risk from foods in contaminated area, Thailand. *Toxicological Research, 32*, 65–72.

Dahaghin, Z., Mousavi, H. Z., & Sajjadi, S. M. (2017). Trace amounts of Cd (II), Cu (II) and Pb (II) ions monitoring using Fe_3O_4@ graphene oxide nanocomposite modified via 2-mercaptobenzothiazole as a novel and efficient nanosorbent. *Journal of Molecular Liquids, 231*, 386–395.

Dargahi, A., Golestanifar, H., Darvishi, P., & Karam, A. (2015). An investigation and comparison of removing heavy metals (lead and chromium) from aqueous solutions using magnesium oxide nanoparticles. *Polish Journal of Environmental Studies, 25*, 557.

Das, G. K., Bonifacio, C. S., De Rojas, J., Liu, K., Van Benthem, K., & Kennedy, I. M. (2014). Ultra-long magnetic nanochains for highly efficient arsenic removal from water. *Journal of Materials Chemistry A, 2*, 12974–12981.

Dastgiri, S., Mosaferi, M., Fizi, M. A., Olfati, N., Zolali, S., Pouladi, N., & Azarfam, P. (2010). Arsenic exposure, dermatological lesions, hypertension, and chromosomal abnormalities among people in a rural community of northwest Iran. *Journal of Health, Population, and Nutrition, 28*, 14.

Daud, M., Khan, Z., Ashgar, A., Danish, M. I., & Qazi, I. A. (2015). Comparing and optimizing nitrate adsorption from aqueous solution using Fe/Pt bimetallic nanoparticles and anion exchange resins. *Journal of Nanotechnology, 2015*, 1.

De Gisi, S., Minetto, D., Lofrano, G., Libralato, G., Conte, B., Todaro, F., & Notarnicola, M. (2017). Nanoscale zero valent iron (nZVI) treatment of marine sediments slightly polluted by heavy metals. *Chemical Engineering Transactions, 60*, 139–144.

Dehaghi, M. (2014). Removal of lead ions from aqueous solution using multi-walled carbon nanotubes: The effect of functionalization. *J. Appl. Environ. Biol. Sci, 4*, 316–326.

Dehghani, M. H., Taher, M. M., Bajpai, A. K., Heibati, B., Tyagi, I., Asif, M., Agarwal, S., & Gupta, V. K. (2015). Removal of noxious Cr (VI) ions using single-walled carbon nanotubes and multi-walled carbon nanotubes. *Chemical Engineering Journal, 279*, 344–352.

Demiral, H., & Güngör, C. (2016). Adsorption of copper (II) from aqueous solutions on activated carbon prepared from grape bagasse. *Journal of Cleaner Production, 124*, 103–113.

Dhandole, L. K., Kim, S.-G., Bae, H.-S., Ryu, H. I., Chung, H.-S., Seo, Y.-S., Cho, M., Shea, P. J., & Jang, J. S. (2020). Simultaneous and synergistic effect of heavy metal adsorption on the enhanced photocatalytic performance of a visible-light-driven RS-TONR/TNT composite. *Environmental Research, 180*, 108651.

Di Natale, F., Gargiulo, V., & Alfè, M. (2020). Adsorption of heavy metals on silica-supported hydrophilic carbonaceous nanoparticles (SHNPs). *Journal of Hazardous Materials, 393*, 122374.

Dietz, K.-J., & Herth, S. (2011). Plant nanotoxicology. *Trends in Plant Science, 16*, 582–589.

Dil, E. A., Asfaram, A., & Sadeghfar, F. (2019a). Magnetic dispersive micro-solid phase extraction with the CuO/ZnO@ Fe 3 O 4-CNTs nanocomposite sorbent for the rapid pre-concentration of chlorogenic acid in the medical extract of plants, food, and water samples. *The Analyst, 144*, 2684–2695.

Dil, E. A., Ghaedi, M., Asfaram, A., & Mehrabi, F. (2017). Application of modificated magnetic nanomaterial for optimization of ultrasound-enhanced removal of Pb^{2+} ions from aqueous solution under experimental design: Investigation of kinetic and isotherm. *Ultrasonics Sonochemistry, 36*, 409–419.

Dil, E. A., Ghaedi, M., Asfaram, A., Mehrabi, F., & Sadeghfar, F. (2019b). Efficient adsorption of Azure B onto CNTs/Zn: ZnO@ Ni_2P-NCs from aqueous solution in the presence of ultrasound wave based on multivariate optimization. *Journal of Industrial and Engineering Chemistry, 74*, 55–62.

Diva, T. N., Zare, K., Taleshi, F., & Yousefi, M. (2017). Synthesis, characterization, and application of nickel oxide/CNT nanocomposites to remove Pb 2+ from aqueous solution. *Journal of Nanostructure in Chemistry, 7*, 273–281.

Dixit, A., Mishra, P., & Alam, M. (2017). Titania nanofibers: A potential adsorbent for mercury and lead uptake. *International Journal of Chemical Engineering and Applications, 8*, 75.

Do, S. Y., Lee, C. G., Kim, J. Y., Moon, Y. H., Kim, M. S., Bae, I. H., & Song, H. S. (2017). Cases of acute mercury poisoning by mercury vapor exposure during the demolition of a fluorescent lamp factory. *Annals of Occupational and Environmental Medicine, 29*, 1–8.

Doggaz, A., Attour, A., Mostefa, M. L. P., Côme, K., Tlili, M., & Lapicque, F. (2019). Removal of heavy metals by electrocoagulation from hydrogenocarbonate-containing waters: Compared cases of divalent iron and zinc cations. *Journal of Water Process Engineering, 29*, 100796.

Dong, L., Hou, L., Wang, Z., Gu, P., Chen, G., & Jiang, R. (2018). A new function of spent activated carbon in BAC process: Removing heavy metals by ion exchange mechanism. *Journal of Hazardous Materials, 359*, 76–84.

Dowlatshahi, S., Haratinezhad Torbati, A. R., & Loloei, M. (2014). Adsorption of copper, lead and cadmium from aqueous solutions by activated carbon prepared from saffron leaves. *Environmental Health Engineering and Management Journal, 1*, 37–44.

Du, Y., Dai, M., Cao, J., & Peng, C. (2019). Fabrication of a low-cost adsorbent supported zero-valent iron by using red mud for removing Pb (II) and Cr (VI) from aqueous solutions. *RSC Advances, 9*, 33486–33496.

Dubinin, M. (1960). The potential theory of adsorption of gases and vapors for adsorbents with energetically nonuniform surfaces. *Chemical Reviews, 60*, 235–241.

Ebadi, M., Shagholani, H., & Jahangiri, H. (2016). High efficient nanocomposite for removal of heavy metals (Hg^{2+} and Pb^{2+}) from aqueous solution. *Journal of Nanostructures*. 6, 23–27.

El-Kafrawy, A. F., El-Saeed, S. M., Farag, R. K., El-Saied, H.A.-A., & Abdel-Raouf, M.E.-S. (2017). Adsorbents based on natural polymers for removal of some heavy metals from aqueous solution. *Egyptian Journal of Petroleum, 26*, 23–32.

El-Khaiary, M. I. (2008). Least-squares regression of adsorption equilibrium data: Comparing the options. *Journal of Hazardous Materials, 158*, 73–87.

El-Sadaawy, M., & Abdelwahab, O. (2014). Adsorptive removal of nickel from aqueous solutions by activated carbons from doum seed (Hyphaenethebaica) coat. *Alexandria Engineering Journal, 53*, 399–408.

El-Shafai, N. M., Abdelfatah, M. M., El-Khouly, M. E., El-Mehasseb, I. M., El-Shaer, A., Ramadan, M. S., Masoud, M. S., & El-Kemary, M. A. (2020). Magnetite nano-spherical quantum dots decorated graphene oxide nano sheet (GO@ Fe_3O_4): Electrochemical properties and applications for removal heavy metals, pesticide and solar cell. *Applied Surface Science, 506*, 144896.

El Haouti, R., Ouachtak, H., El Guerdaoui, A., Amedlous, A., Amaterz, E., Haounati, R., Addi, A. A., Akbal, F., El Alem, N., & Taha, M. L. (2019). Cationic dyes adsorption by Na-Montmorillonite Nano Clay: Experimental study combined with a theoretical investigation using DFT-based descriptors and molecular dynamics simulations. *Journal of Molecular Liquids, 290*, 111139.

Elbana, T. A., Selim, H. M., Akrami, N., Newman, A., Shaheen, S. M., & Rinklebe, J. (2018). Freundlich sorption parameters for cadmium, copper, nickel, lead, and zinc for different soils: Influence of kinetics. *Geoderma, 324*, 80–88.

Elhami, S., & Shafizadeh, S. (2016). Removal of Mercury (II) using modified Nanoclay. *Materials Today: Proceedings, 3*, 2623–2627.

Elkady, M., Hussein, M., & Atiaa, H. (2015). Preparation of nano-activated carbon from carbon based material for copper decontamination from wastewater. *Am. J. Appl. Chem, 3*, 31–37.

Odey E. A, A. S. G., & Harrison Ikhumhen. (2017). Borehole Water Quality Assessment in Bekwarra, Nigeria. *Advances in Recycling & Waste Management*. 2(1).

Engates, K. E., & Shipley, H. J. (2011). Adsorption of Pb, Cd, Cu, Zn, and Ni to titanium dioxide nanoparticles: Effect of particle size, solid concentration, and exhaustion. *Environmental Science and Pollution Research, 18*, 386–395.

Esquinas-Requena, J. L., Lozoya-Moreno, S., García-Nogueras, I., Atienzar-Núñez, P., Sánchez-Jurado, P. M., & Abizanda, P. (2020). La anemia aumenta el riesgo de mortalidad debido a fragilidad y discapacidad en mayores: Estudio FRADEA. *Atención Primaria, 52*, 452–461.

Fard, R. F., Sar, M. E. K., Fahiminia, M., Mirzaei, N., Yousefi, N., Mansoorian, H. J., Khanjani, N., Rezaei, S., Ghadiri, S. K. (2018). Efficiency of multi walled carbon nanotubes for removing Direct Blue 71 from aqueous solutions. *Eurasian Journal of Analytical Chemistry, 13*(3), 123–146.

Farghali, A., Bahgat, M., Allah, A. E., & Khedr, M. (2013). Adsorption of Pb (II) ions from aqueous solutions using copper oxide nanostructures. *Beni-Suef University Journal of Basic and Applied Sciences, 2*, 61–71.

Farid, M. U., Luan, H.-Y., Wang, Y., Huang, H., An, A. K., & Khan, R. J. (2017). Increased adsorption of aqueous zinc species by Ar/O_2 plasma-treated carbon nanotubes immobilized in hollow-fiber ultrafiltration membrane. *Chemical Engineering Journal, 325*, 239–248.

Farooghi, A., Sayadi, M. H., Rezaei, M. R., & Allahresani, A. (2018). An efficient removal of lead from aqueous solutions using $FeNi_3$@ SiO_2 magnetic nanocomposite. *Surfaces and Interfaces, 10*, 58–64.

Fashola, M. O., Ngole-Jeme, V. M., & Babalola, O. O. (2016). Heavy metal pollution from gold mines: Environmental effects and bacterial strategies for resistance. *International Journal of Environmental Research and Public Health, 13*, 1047.

Fonseca-Correa, R. A., Giraldo, L., & Moreno-Piraján, J. C. (2019). Thermodynamic study of adsorption of nickel ions onto carbon aerogels. *Heliyon, 5*, e01789.

Foo, K., & Hameed, B. (2012). Preparation, characterization and evaluation of adsorptive properties of orange peel based activated carbon via microwave induced K_2CO_3 activation. *Bioresource Technology, 104*, 679–686.

Gaffer, A., Al Kahlawy, A. A., & Aman, D. (2017). Magnetic zeolite-natural polymer composite for adsorption of chromium (VI). *Egyptian Journal of Petroleum, 26*, 995–999.

Gangadhar, G., Maheshwari, U., & Gupta, S. (2012). Application of nanomaterials for the removal of pollutants from effluent streams. *Nanoscience & Nanotechnology-Asia, 2*, 140–150.

Gao, F., Gu, H., Wang, H., Wang, X., Xiang, B., & Guo, Z. (2015). Magnetic amine-functionalized polyacrylic acid-nanomagnetite for hexavalent chromium removal from polluted water. *RSC Advances, 5*, 60208–60219.

Gardner, S. (2009). *Fate, transport, and bioavailability of arsenic in manured and contaminated soils of Delaware*. University of Delaware.

Gautam, P. K., Gautam, R. K., Banerjee, S., Chattopadhyaya, M., & Pandey, J. (2016). Heavy metals in the environment: Fate, transport, toxicity and remediation technologies. *Nova Sci Publishers, 60*, 101–130.

Ge, L., Wang, W., Peng, Z., Tan, F., Wang, X., Chen, J., & Qiao, X. (2018). Facile fabrication of Fe@ MgO magnetic nanocomposites for efficient removal of heavy metal ion and dye from water. *Powder Technology, 326*, 393–401.

Ghaniem, R., El-Taweil, Y., & Ossman, M. (2016). Use of hydrous manganese oxides nanopowders as a potential sorbent for selective removal of nickel ions from industrial waste water, kinetics and isotherm studies. *American Journal of Chemical Engineering, 4*, 170–178.

Ghorbani, M., Eisazadeh, H., & Ghoreyshi, A. (2012). Removal of zinc ions from aqueous solution using polyaniline nanocomposite coated on rice husk. *Iranica Journal of Energy & Environment, 3*, 83–88.

Giraldo, L., Erto, A., & Moreno-Piraján, J. C. (2013). Magnetite nanoparticles for removal of heavy metals from aqueous solutions: Synthesis and characterization. *Adsorption, 19*, 465–474.

Golkhah, S., Zavvar, M. H., Shirkhanloo, H., & Khaligh, A. (2017). Removal of Pb (II) and Cu (II) ions from aqueous solutions by cadmium sulfide nanoparticles. *International Journal of Nanoscience and Nanotechnology*,13(2), 105–117.

Gómez Pastora, J., Bringas Elizalde, E., & Ortiz Uribe, I. (2016). Design of novel adsorption processes for the removal of arsenic from polluted groundwater employing functionalized magnetic nanoparticles. *Chemical Engineering Transactions*, 47, 241–246.

Gunatilake, S. (2015). Methods of removing heavy metals from industrial wastewater. *Methods, 1*, 14.

Guo, T., Bulin, C., Li, B., Zhao, Z., Yu, H., Sun, H., Ge, X., Xing, R., & Zhang, B. (2018). Efficient removal of aqueous Pb (II) using partially reduced graphene oxide-Fe_3O_4. *Adsorption Science & Technology, 36*, 1031–1048.

Gupta, N., Kushwaha, A. K., & Chattopadhyaya, M. (2016). Application of potato (*Solanum tuberosum*) plant wastes for the removal of methylene blue and malachite green dye from aqueous solution. *Arabian Journal of Chemistry, 9*, S707–S716.

Hameed, A. K., Dewayanto, N., Dongyun, D., Nordin, M. R., & Ab Rahim, M. H. (2016). Kinetic and thermodynamics of methylene blue adsorption onto zero valent iron supported on mesoporous silica. *Bulletin of Chemical Reaction Engineering & Catalysis, 11*, 250–261.

Hänsch, R., & Mendel, R. R. (2009). Physiological functions of mineral micronutrients (cu, Zn, Mn, Fe, Ni, Mo, B, cl). *Current Opinion in Plant Biology, 12*, 259–266.

Hao, Y.-M., Man, C., & Hu, Z.-B. (2010). Effective removal of Cu (II) ions from aqueous solution by amino-functionalized magnetic nanoparticles. *Journal of Hazardous Materials, 184*, 392–399.

Hekmatzadeh, A., Karimi-Jashani, A., & Talebbeydokhti, N. (2012). Mass transfer modeling of nitrate in an ion exchange selective resin. *International Journal of Civil and Environmental Engineering, 6*, 58–63.

Hernández-Flores, H., Pariona, N., Herrera-Trejo, M., Hdz-García, H. M., & Mtz-Enriquez, A. I. (2018). Concrete/maghemite nanocomposites as novel adsorbents for arsenic removal. *Journal of Molecular Structure, 1171*, 9–16.

Homaeigohar, S. (2020). The nanosized dye adsorbents for water treatment. *Nanomaterials, 10*, 295.

Hossini, H., Rezaee, A., & Mohamadiyan, G. (2015). Hexavalent chromium removal from aqueous solution using functionalized multi-walled carbon nanotube: Optimization of parameters by response surface methodology. *Health Scope, 4*(1), 19892.

Huang, B., Qi, C., Yang, Z., Guo, Q., Chen, W., Zeng, G., & Lei, C. (2017). Pd/Fe_3O_4 nanocatalysts for highly effective and simultaneous removal of humic acids and Cr (VI) by electro-Fenton with H_2O_2 in situ electro-generated on the catalyst surface. *Journal of Catalysis, 352*, 337–350.

Huang, D.-L., Chen, G.-M., Zeng, G.-M., Xu, P., Yan, M., Lai, C., Zhang, C., Li, N.-J., Cheng, M., & He, X.-X. (2015). Synthesis and application of modified zero-valent iron nanoparticles for removal of hexavalent chromium from wastewater. *Water, Air, & Soil Pollution, 226*, 1–14.

Huang, S., Ma, C., Liao, Y., Min, C., Du, P., & Jiang, Y. (2016). Removal of mercury (II) from aqueous solutions by adsorption on poly (1-amino-5-chloroanthraquinone) nanofibrils: Equilibrium, kinetics, and mechanism studies. *Journal of Nanomaterials, 2016*, 1.

Imchuen, N., Lubphoo, Y., Chyan, J.-M., Padungthon, S., & Liao, C.-H. (2016). Using cation exchange resin for ammonium removal as part of sequential process for nitrate reduction by nanoiron. *Sustainable Environment Research, 26*, 156–160.

Izbicki, J. A., Ball, J. W., Bullen, T. D., & Sutley, S. J. (2008). Chromium, chromium isotopes and selected trace elements, western Mojave Desert, USA. *Applied Geochemistry, 23*, 1325–1352.

Jagaba, A., Kutty, S., Khaw, S., Lai, C., Isa, M., Baloo, L., Lawal, I., Abubakar, S., Umaru, I., & Zango, Z. (2020). Derived hybrid biosorbent for zinc (II) removal from aqueous solution by continuous-flow activated sludge system. *Journal of Water Process Engineering, 34*, 101152.

Jetty, P., Jayaram, S., Veinot, J., & Pratt, M. (2013). Superficial femoral artery nitinol stent in a patient with nickel allergy. *Journal of Vascular Surgery, 58*, 1388–1390.

Jia, Z., Shu, Y., Huang, R., Liu, J., & Liu, L. (2018). Enhanced reactivity of nZVI embedded into supermacroporous cryogels for highly efficient Cr (VI) and total Cr removal from aqueous solution. *Chemosphere, 199*, 232–242.

Jin, Z., Deng, S., Wen, Y., Jin, Y., Pan, L., Zhang, Y., Black, T., Jones, K. C., Zhang, H., & Zhang, D. (2019). Application of Simplicillium chinense for Cd and Pb biosorption and enhancing heavy metal phytoremediation of soils. *Science of the Total Environment, 697*, 134148.

Julkapli, N. M., Bagheri, S., & Sapuan, S. (2015). *Multifunctionalized carbon nanotubes polymer composites: Properties and applications. Eco-friendly polymer nanocomposites* (pp. 155–214). Springer, New Delhi. 155-214.

Kakaei, A. (2016). Removal of Cd (II) in water samples using modified magnetic iron oxide nanoparticle. *Iranian Journal of Toxicology, 10*, 9–14.

Kalantari, K., Ahmad, M. B., Masoumi, H. R. F., Shameli, K., Basri, M., & Khandanlou, R. (2014). Rapid adsorption of heavy metals by Fe_3O_4/talc nanocomposite and optimization study using response surface methodology. *International Journal of Molecular Sciences, 15*, 12913–12927.

Kapinder, D. M., Verma, A. K. (2017). Exploiting the Potential of Nanotechnological Applications in Rural Areas to Effectively Eliminate Pollutants from Water Bodies. J. Pharm. Res, 11.

Karnib, M., Kabbani, A., Holail, H., & Olama, Z. (2014). Heavy metals removal using activated carbon, silica and silica activated carbon composite. *Energy Procedia, 50*, 113–120.

Kaveeshwar, A. R., Ponnusamy, S. K., Revellame, E. D., Gang, D. D., Zappi, M. E., & Subramaniam, R. (2018). Pecan shell based activated carbon for removal of iron (II) from fracking wastewater:

Adsorption kinetics, isotherm and thermodynamic studies. *Process Safety and Environmental Protection, 114*, 107–122.

Keyhanian, F., Shariati, S., Faraji, M., & Hesabi, M. (2016). Magnetite nanoparticles with surface modification for removal of methyl violet from aqueous solutions. *Arabian Journal of Chemistry, 9*, S348–S354.

Khatoon, N., Khan, A. H., Pathak, V., Agnihotri, N., & Rehman, M. (2013). Removal of hexavalent chromium from synthetic waste water using synthetic nano zero valent iron (NZVI) as adsorbent. *International Journal of Innovative Research in Science, Engineering and Technology, 2*, 2319–8753.

Khazaei, M., Nasseri, S., Ganjali, M. R., Khoobi, M., Nabizadeh, R., Mahvi, A. H., Nazmara, S., & Gholibegloo, E. (2016). Response surface modeling of lead (II) removal by graphene oxide-Fe_3O_4 nanocomposite using central composite design. *Journal of Environmental Health Science and Engineering, 14*, 1–14.

Khodadadi, M., Ehrampoush, M. H., Mahvi, A. H., Dorri, H., Rafati, L., & Naghizadeh, A. (2015). Preparation of magnetic chitosan/Fe-Zr nanoparticles for the removal of heavy metals from aqueous solution. *Journal of Advances in Environmental Health Research, 3*, 266–275.

Kim, S. A., Kamala-Kannan, S., Lee, K.-J., Park, Y.-J., Shea, P. J., Lee, W.-H., Kim, H.-M., & Oh, B.-T. (2013). Removal of Pb (II) from aqueous solution by a zeolite–nanoscale zero-valent iron composite. *Chemical Engineering Journal, 217*, 54–60.

Kiran, S., Adeel, S., Rehman, F. U., Gulzar, T., Jannat, M., & Zuber, M. (2019). Ecofriendly dyeing of microwave treated cotton fabric using reactive violet H3R. *Global Nest Journal, 21*, 43–47.

Konczyk, J., Kozlowski, C., & Walkowiak, W. (2013). Lead (II) removal from aqueous solutions by solvent extraction with tetracarboxylresorcin [4] arene. *Physicochemical Problems of Mineral Processing, 49*, 213–222.

Kosa, S. A., Al-Zhrani, G., & Salam, M. A. (2012). Removal of heavy metals from aqueous solutions by multi-walled carbon nanotubes modified with 8-hydroxyquinoline. *Chemical Engineering Journal, 181*, 159–168.

Kumar, P. S., Saravanan, A., & Yashwanthraj, M. (2017). Nanoscale zero-valent iron-impregnated agricultural waste as an effective biosorbent for the removal of heavy metal ions from wastewater. *Textiles and Clothing Sustainability, 2*, 1–11.

Langsch, J. E., Costa, M., Moore, L., Morais, P., Bellezza, A., & Falcão, S. (2012). New technology for arsenic removal from mining effluents. *Journal of Materials Research and Technology, 1*, 178–181.

Larakeb, M., Youcef, L., & Achour, S. (2017). Removal of zinc from water by adsorption on bentonite and kaolin. *Athens J Sci, 4*, 47–57.

Leonard, A., & Lauwerys, R. (1980). Carcinogenicity and mutagenicity of chromium. *Mutation Research/reviews in Genetic Toxicology, 76*, 227–239.

Leslie, K. E., & Koger, S. M. (2011). A significant factor in autism: Methyl mercury induced oxidative stress in genetically susceptible individuals. *Journal of Developmental and Physical Disabilities, 23*, 313–324.

Li, H., Ding, Z., Fang, J., Gao, Y., & Sun, C. (2014). Effects of annealing process on microstructure and electrical properties of cold-drawn thin layer copper cladding steel wire. *Journal of Materials Science: Materials in Electronics, 25*, 5107–5113.

Li, X., Dou, X., & Li, J. (2012). Antimony (V) removal from water by iron-zirconium bimetal oxide: Performance and mechanism. *Journal of Environmental Sciences, 24*, 1197–1203.

Li, Y., Gai, T., Shao, L., Tang, H., Li, R., Yang, S., Wang, S., Wu, Q., & Ren, Y. (2019). Synthesis of sandwich-like Mn_3O_4@ reduced graphene oxide nano-composites via modified Hummers' method and its application as uranyl adsorbents. *Heliyon, 5*, e01972.

Liang, W., Dai, C., Zhou, X., & Zhang, Y. (2014). Application of zero-valent iron nanoparticles for the removal of aqueous zinc ions under various experimental conditions. *PLoS ONE, 9*, e85686.

Liu, S., Chen, M., Cao, X., Li, G., Zhang, D., Li, M., Meng, N., Yin, J., & Yan, B. (2020a). Chromium (VI) removal from water using cetylpyridinium chloride (CPC)-modified montmorillonite. *Separation and Purification Technology, 241*, 116732.

Liu, X., Guan, J., Lai, G., Xu, Q., Bai, X., Wang, Z., & Cui, S. (2020b). Stimuli-responsive adsorption behavior toward heavy metal ions based on comb polymer functionalized magnetic nanoparticles. *Journal of Cleaner Production, 253*, 119915.

Lobo, V., Patil, A., Phatak, A., & Chandra, N. (2010). Removal of Nickel (II) from Aqueous Solution by adsorption onto Nano adsorbent prepared from Cucumis Melo peel. *Pharmacognosy Reviews, 4*, 118–126.

Ma, H., Yang, J., Gao, X., Liu, Z., Liu, X., & Xu, Z. (2019). Removal of chromium (VI) from water by porous carbon derived from corn straw: Influencing factors, regeneration and mechanism. *Journal of Hazardous Materials, 369*, 550–560.

Madala, S., Nadavala, S. K., Vudagandla, S., Boddu, V. M., & Abburi, K. (2017). Equilibrium, kinetics and thermodynamics of Cadmium (II) biosorption on to composite chitosan biosorbent. *Arabian Journal of Chemistry, 10*, S1883–S1893.

Madivoli, E., Kareru, P., Gachanja, A., Mugo, S., Murigi, M., Kairigo, P., Kipyegon, C., Mutembei, J., Njonge, F. (2016). Adsorption of selected heavy metals on modified nano cellulose. *International Research Journal of Pure and Applied Chemistry*, 12, 1–9.

Madzokere, T. C., & Karthigeyan, A. (2017). Heavy metal ion effluent discharge containment using magnesium oxide (MgO) nanoparticles. *Materials Today: Proceedings, 4*, 9–18.

Mahmood, S. A. I. (2012). Impact of climate change in Bangladesh: The role of public administration and governments integrity. *Journal of Ecology and the Natural Environment, 4*, 223–240.

Mahmoud, A. M., Ibrahim, F. A., Shaban, S. A., & Youssef, N. A. (2015). Adsorption of heavy metal ion from aqueous solution by nickel oxide nano catalyst prepared by different methods. *Egyptian Journal of Petroleum, 24*, 27–35.

Mahmoudian, S. (2019). Removal of cationic dyes from aqueous solution using organomodified nanoclay. *Int. J. Bio-Inorg. Hybr. Nanomater, 8*, 95–99.

Mahurpawar, M. (2015). Effects of heavy metals on human health. *International Journal of Research-Granthaalayah, 3*, 1–7.

Malayoglu, U. (2018). Removal of heavy metals by biopolymer (chitosan)/nanoclay composites. *Separation Science and Technology, 53*, 2741–2749.

Manal, L., & Leila, Y. (2016). Removal of zinc from water by adsorption on different adsorbent. *Journal of New Technology and Materials, 6*, 19–25.

Mandal, P., Debbarma, S., Saha, A., & Ruj, B. (2016). Disposal problem of arsenic sludge generated during arsenic removal from drinking water. *Procedia Environmental Sciences, 35*, 943–949.

Mandal, S., Sahu, M. K., & Patel, R. K. (2013). Adsorption studies of arsenic (III) removal from water by zirconium polyacrylamide hybrid material (ZrPACM-43). *Water Resources and Industry, 4*, 51–67.

Manyangadze, M., Chikuruwo, N. M., Narsaiah, T. B., Chakra, C. S., Charis, G., Danha, G., & Mamvura, T. A. (2020). Adsorption of lead ions from wastewater using nano silica spheres synthesized on calcium carbonate templates. *Heliyon, 6*, e05309.

Meena, A. K., Kadirvelu, K., Mishraa, G., Rajagopal, C., & Nagar, P. (2008). Adsorption of Pb (II) and Cd (II) metal ions from aqueous solutions by mustard husk. *Journal of Hazardous Materials, 150*, 619–625.

Mehdizadeh, S., Sadjadi, S., Ahmadi, S. J., & Outokesh, M. (2014). Removal of heavy metals from aqueous solution using platinum nanopartcles/Zeolite-4A. *Journal of Environmental Health Science and Engineering, 12*, 1–7.

Meira, S. M. M., Jardim, A. I., & Brandelli, A. (2015). Adsorption of nisin and pediocin on nanoclays. *Food Chemistry, 188*, 161–169.

Mikulášek, P., & Cuhorka, J. (2016). Removal of heavy metal ions from aqueous solutions by nanofiltration. In *International Conference on Nanotechnology Based Innovative Applications for the Environment*. AIDIC Servizi srl. 47, 379–384.

Mobasherpour, I., Salahi, E., & Ebrahimi, M. (2014). Thermodynamics and kinetics of adsorption of Cu (II) from aqueous solutions onto multi-walled carbon nanotubes. *Journal of Saudi Chemical Society, 18*, 792–801.

Moersidik, S. S., Nugroho, R., Handayani, M., & Pratama, M. A. (2020). Optimization and reaction kinetics on the removal of Nickel and COD from wastewater from electroplating industry using Electrocoagulation and Advanced Oxidation Processes. *Heliyon, 6*, e03319.

Mohammed, A. A. (2015). Biosynthesis and size of silver nanoparticles using *Aspergillus niger* ATCC 16404 as antibacterial activity. *International Journal of Current Microbiology and Applied Sciences, 4*, 522–528.

Mojoudi, F., Hamidian, A. H., Zhang, Y., & Yang, M. (2019). Synthesis and evaluation of activated carbon/nanoclay/thiolated graphene oxide nanocomposite for lead (II) removal from aqueous solution. *Water Science and Technology, 79*, 466–479.

Molaei, K., Bagheri, H., Asgharinezhad, A. A., Ebrahimzadeh, H., & Shamsipur, M. (2017). SiO_2-coated magnetic graphene oxide modified with polypyrrole–polythiophene: A novel and efficient nanocomposite for solid phase extraction of trace amounts of heavy metals. *Talanta, 167*, 607–616.

Moore, M. (2006). Do nanoparticles present ecotoxicological risks for the health of the aquatic environment? *Environment International, 32*, 967–976.

Mousavi, S. A., Almasi, A., Navazeshkha, F., & Falahi, F. (2019). Biosorption of lead from aqueous solutions by algae biomass: Optimization and modeling. *Desalination and Water Treatment, 148*, 229–237.

Mousavi, S. A., & Janjani, H. (2018). Antibiotics adsorption from aqueous solutions using carbon nanotubes: a systematic review. *Toxin Reviews*, 1–12.

Mousavi, S. A., Zangeneh, H., Almasi, A., Nayeri, D., Monkaresi, M., Mahmoudi, A., & Darvishi, P. (2020). Decolourization of aqueous Methylene Blue solutions by corn stalk: modeling and optimization. *Desalin and Water Treatment, 197*, 335.

Mthombeni, N. H., Mbakop, S., & Onyango, M. S. (2015). Magnetic zeolite-polymer composite as an adsorbent for the remediation of wastewaters containing vanadium. *International Journal of Environmental Science and Development, 6*, 602.

Mubarak, N. M., Sahu, J. N., Abdullah, E. C., & Jayakumar, N. S. (2016). Rapid adsorption of toxic Pb (II) ions from aqueous solution using multiwall carbon nanotubes synthesized by microwave chemical vapor deposition technique. *Journal of Environmental Sciences, 45*, 143–155.

Nadia Moustafa Ahmed, N. M. (2015). Synthesis and characterization of zinc oxide nano particles for the removal of Cr (VI). *International Journal of Scientific & Engineering Research, 6*, 1235–1243.

Nanta, P., Kasemwong, K., & Skolpap, W. (2018). Isotherm and kinetic modeling on superparamagnetic nanoparticles adsorption of polysaccharide. *Journal of Environmental Chemical Engineering, 6*, 794–802.

Nasrullah, A., Bhat, A., Naeem, A., Isa, M. H., & Danish, M. (2018). High surface area mesoporous activated carbon-alginate beads for efficient removal of methylene blue. *International Journal of Biological Macromolecules, 107*, 1792–1799.

Nayeri, D., & Mousavi, S. A. (2020a). Dye removal from water and wastewater by nanosized metal oxides-modified activated carbon: a review on recent researches. *Journal of Environmental Health Science and Engineering*, 18(2),1671–1689.

Nayeri, D., & Mousavi, S. A. (2020b). Treatment of highly turbid water in disaster conditions using coagulation-flocculation process: Modeling and optimization. *Water Quality Research Journal, 55*, 358–369.

Nayeri, D., Mousavi, S. A., & Mehrabi, A. (2019). Oxytetracycline removal from aqueous solutions using activated carbon prepared from corn stalks. *Journal of Applied Research in Water and Wastewater, 6*, 67–72.

Nayeria, D., Mousavia, S. A., Darvishia, P., Mahmoudia, A., Nooria, E., & Delavaric, S. (2019). Evaluation of water quality and stability in the drinking water distribution network: A case study in the Kermanshah city. *Iran. Desalination and Water Treatment, 166*, 180–185.

Nemati, M., Hosseini, S., & Shabanian, M. (2017). Novel electrodialysis cation exchange membrane prepared by 2-acrylamido-2-methylpropane sulfonic acid; heavy metal ions removal. *Journal of Hazardous Materials, 337*, 90–104.

Nethaji, S., Sivasamy, A., & Mandal, A. (2013). Adsorption isotherms, kinetics and mechanism for the adsorption of cationic and anionic dyes onto carbonaceous particles prepared from Juglans regia shell biomass. *International Journal of Environmental Science and Technology, 10*, 231–242.

Nguyen, B. T., Do, D. D., Nguyen, T. X., Nguyen, V. N., Nguyen, D. T. P., Nguyen, M. H., Truong, H. T. T., Dong, H. P., Le, A. H., & Bach, Q.-V. (2020). Seasonal, spatial variation, and pollution sources of heavy metals in the sediment of the Saigon River. *Vietnam. Environmental Pollution, 256*, 113412.

Njoku, V., Foo, K., Asif, M., & Hameed, B. (2014). Preparation of activated carbons from rambutan (*Nephelium lappaceum*) peel by microwave-induced KOH activation for acid yellow 17 dye adsorption. *Chemical Engineering Journal, 250*, 198–204.

Nur, T., Shim, W., Loganathan, P., Vigneswaran, S., & Kandasamy, J. (2015). Nitrate removal using Purolite A520E ion exchange resin: Batch and fixed-bed column adsorption modelling. *International Journal of Environmental Science and Technology, 12*, 1311–1320.

Obayomi, K., Bello, J., Yahya, M. D., Chukwunedum, E., & Adeoye, J. (2020). Statistical analyses on effective removal of cadmium and hexavalent chromium ions by multiwall carbon nanotubes (MWCNTs). *Heliyon, 6*, e04174.

Ociński, D., Jacukowicz-Sobala, I., Mazur, P., Raczyk, J., & Kociołek-Balawejder, E. (2016). Water treatment residuals containing iron and manganese oxides for arsenic removal from water–characterization of physicochemical properties and adsorption studies. *Chemical Engineering Journal, 294*, 210–221.

Ojedokun, A. T., & Bello, O. S. (2016). Sequestering heavy metals from wastewater using cow dung. *Water Resources and Industry, 13*, 7–13.

Okpala, C. C. (2014). The benefits and applications of nanocomposites. *International Journal of Advanced Engineering and Technology, 4*, 12–18.

Omraei, M., Esfandian, H., Katal, R., & Ghorbani, M. (2011). Study of the removal of Zn (II) from aqueous solution using polypyrrole nanocomposite. *Desalination, 271*, 248–256.

Oprčkal, P., Mladenovič, A., Vidmar, J., Pranjić, A. M., Milačič, R., & Ščančar, J. (2017). Critical evaluation of the use of different nanoscale zero-valent iron particles for the treatment of effluent water from a small biological wastewater treatment plant. *Chemical Engineering Journal, 321*, 20–30.

Ozairi, N., Mousavi, S. A., Samadi, M. T., Seidmohammadi, A., & Nayeri, D. (2020). Removal of fluoride from water using coagulation–flocculation procea comparative study. *Desalination and Water Treatment, 180*, 265–270.

Padmavathy, K., Madhu, G., & Haseena, P. (2016). A study on effects of pH, adsorbent dosage, time, initial concentration and adsorption isotherm study for the removal of hexavalent chromium (Cr (VI)) from wastewater by magnetite nanoparticles. *Procedia Technology, 24*, 585–594.

Panji, A., Simha, L. U., & Nagabhushana, B. (2016). Heavy metals removal by nickel-oxide nanoparticles synthesised by lemon juice extract. *International Journal of Engineering and Management Research (IJEMR), 6*, 287–291.

Pardo, A., Pelaz, B., del Pino, P., Al-Modlej, A., Cambón, A., Velasco, B., Domínguez-González, R., Moreda-Piñeiro, A., Bermejo-Barrera, P., & Barbosa, S. (2021). Monodisperse superparamagnetic nanoparticles separation adsorbents for high-yield removal of arsenic and/or mercury metals in aqueous media. *Journal of Molecular Liquids, 335*, 116485.

Park, J.-D., & Zheng, W. (2012). Human exposure and health effects of inorganic and elemental mercury. *Journal of Preventive Medicine and Public Health, 45*, 344.

Patel, H. A., Somani, R. S., Bajaj, H. C., & Jasra, R. V. (2006). Nanoclays for polymer nanocomposites, paints, inks, greases and cosmetics formulations, drug delivery vehicle and waste water treatment. *Bulletin of Materials Science, 29*, 133–145.

Patil, C. S., Gunjal, D. B., Naik, V. M., Harale, N. S., Jagadale, S. D., Kadam, A. N., Patil, P. S., Kolekar, G. B., & Gore, A. H. (2019). Waste tea residue as a low cost adsorbent for removal of hydralazine hydrochloride pharmaceutical pollutant from aqueous media: An environmental remediation. *Journal of Cleaner Production, 206*, 407–418.

Pekey, H. (2006). The distribution and sources of heavy metals in Izmit Bay surface sediments affected by a polluted stream. *Marine Pollution Bulletin, 52*, 1197–1208.

Pietrzak, K. J. a. R. (2013). Metals Ions Removal by Polymer Membranes of Different Porosity. *The Scientific World Journal*. 2013.

Pillai, P., Kakadiya, N., Timaniya, Z., Dharaskar, S., & Sillanpaa, M. (2020). Removal of arsenic using iron oxide amended with rice husk nanoparticles from aqueous solution. *Materials Today: Proceedings, 28*, 830–835.

Pirbazari, A. E., Saberikhah, E., & Kozani, S. H. (2014). Fe_3O_4–wheat straw: Preparation, characterization and its application for methylene blue adsorption. *Water Resources and Industry, 7*, 23–37.

Pourrut, B., Shahid, M., Dumat, C., Winterton, P., & Pinelli, E. (2011). Lead uptake, toxicity, and detoxification in plants. *Reviews of Environmental Contamination and Toxicology, 213*, 113–136.

Poursani, A. S., Nilchi, A., Hassani, A., Shariat, S. M., & Nouri, J. (2016). The synthesis of nano TiO_2 and its use for removal of lead ions from aqueous solution. *Journal of Water Resource and Protection, 8*, 438.

Pradhan, S. K., Panwar, J., & Gupta, S. (2017). Enhanced heavy metal removal using silver-yttrium oxide nanocomposites as novel adsorbent system. *Journal of Environmental Chemical Engineering, 5*, 5801–5814.

Prajapati, A. K., & Mondal, M. K. (2020). Comprehensive kinetic and mass transfer modeling for methylene blue dye adsorption onto CuO nanoparticles loaded on nanoporous activated carbon prepared from waste coconut shell. *Journal of Molecular Liquids, 307*, 112949.

Qiao, D., Wang, G., Li, X., Wang, S., & Zhao, Y. (2020). Pollution, sources and environmental risk assessment of heavy metals in the surface AMD water, sediments and surface soils around unexploited Rona Cu deposit, Tibet. *China. Chemosphere, 248*, 125988.

Qu, G., Kou, L., Wang, T., Liang, D., & Hu, S. (2017). Evaluation of activated carbon fiber supported nanoscale zero-valent iron for chromium (VI) removal from groundwater in a permeable reactive column. *Journal of Environmental Management, 201*, 378–387.

Rachmawati, S. D., Tizaoui, C., & Hilal, N. (2013). Manganese coated sand for copper (II) removal from water in batch mode. *Water, 5*, 1487–1501.

Rahmani, A., Ghaffari, H., & Samadi, M. (2010). Removal of arsenic (III) from contaminated water by synthetic nano size zerovalent iron. *World Academy of Science, Engineering and Technology, 62*, 737–740.

Ramesh, S., Rameshbabu, N., Gandhimathi, R., Kumar, M. S., & Nidheesh, P. (2013). Adsorptive removal of Pb (II) from aqueous solution using nano-sized hydroxyapatite. *Applied Water Science, 3*, 105–113.

Rashid, J., Azam, R., Kumar, R., Ahmad, M., Rehman, A., & Barakat, M. (2019). Sulfonated polyether sulfone reinforced multiwall carbon nanotubes composite for the removal of lead in wastewater. *Applied Nanoscience, 9*, 1695–1705.

Ray, P. C., Yu, H., & Fu, P. P. (2009). Toxicity and environmental risks of nanomaterials: Challenges and future needs. *Journal of Environmental Science and Health Part C, 27*, 1–35.

Razmgar, K., & Mokhtari Hosseini, Z. B. (2016). Removal of As (V), Cr (VI) and Pb (II) from aqueous solution using surfactant-modified *Sabzevar nanozeolite*. *Advances in Environmental Technology, 2*, 105–109.

Reddy, S., Nirmala, V., & Ashwini, C. (2014). Bengal gram seed husk as an adsorbent for the removal of dye from aqueous solutions-batch studies. *Arabian Journal of Chemistry*, 1–12.

Rubio, J., Souza, M., & Smith, R. (2002). Overview of flotation as a wastewater treatment technique. *Minerals Engineering, 15*, 139–155.

Ruparelia, J., Duttagupta, S., Chatterjee, A., & Mukherji, S. (2008). Potential of carbon nanomaterials for removal of heavy metals from water. *Desalination, 232*, 145–156.

Salam, E. A., Abou El-Nour, K., Awad, A., & Orabi, A. (2020). Carbon nanotubes modified with 5, 7-dinitro-8-quinolinol as potentially applicable tool for efficient removal of industrial wastewater pollutants. *Arabian Journal of Chemistry, 13*, 109–119.

Salam, M. A. (2013). Removal of heavy metal ions from aqueous solutions with multi-walled carbon nanotubes: Kinetic and thermodynamic studies. *International Journal of Environmental Science and Technology, 10*, 677–688.

Salam, M. A., Alshehri, A. A., Schwieger, W., & Mokhtar, M. (2021). Removal of bismuth ions utilizing pillared ilerite nanoclay: Kinetic thermodynamic studies and environmental application. *Microporous and Mesoporous Materials, 313*, 110826.

Salam, M. A., Kosa, S. A., & Al-Beladi, A. A. (2017). Application of nanoclay for the adsorptive removal of Orange G dye from aqueous solution. *Journal of Molecular Liquids, 241*, 469–477.

Salam, O. E. A., Reiad, N. A., & ElShafei, M. M. (2011). A study of the removal characteristics of heavy metals from wastewater by low-cost adsorbents. *Journal of Advanced Research, 2*, 297–303.

Salem, I. A., Salem, M. A., & El-Ghobashy, M. A. (2017). The dual role of ZnO nanoparticles for efficient capture of heavy metals and Acid blue 92 from water. *Journal of Molecular Liquids, 248*, 527–538.

Shafiabadi, M., Dashti, A., & Tayebi, H.-A. (2016). Removal of Hg (II) from aqueous solution using polypyrrole/SBA-15 nanocomposite: Experimental and modeling. *Synthetic Metals, 212*, 154–160.

Shahbazi, D., Mousavi, S., & Nayeri, D. (2020). Low-cost activated carbon: Characterization, decolorization, modeling, optimization and kinetics. *International Journal of Environmental Science and Technology, 17*, 3935–3946.

Shahriari, T., Bidhendi, G. N., Mehrdadi, N., & Torabian, A. (2014). Effective parameters for the adsorption of chromium (III) onto iron oxide magnetic nanoparticle. *International Journal of Environmental Science and Technology, 11*, 349–356.

Shaibu, S. E., Adekola, F. A., Adegoke, H. I., & Ayanda, O. S. (2014). A comparative study of the adsorption of methylene blue onto synthesized nanoscale zero-valent iron-bamboo and manganese-bamboo composites. *Materials, 7*, 4493–4507.

Shan, R., Shi, Y., Gu, J., Wang, Y., & Yuan, H. (2020). Single and competitive adsorption affinity of heavy metals toward peanut shell-derived biochar and its mechanisms in aqueous systems. *Chinese Journal of Chemical Engineering, 28*, 1375–1383.

Shang, J., Zong, M., Yu, Y., Kong, X., Du, Q., & Liao, Q. (2017). Removal of chromium (VI) from water using nanoscale zerovalent iron particles supported on herb-residue biochar. *Journal of Environmental Management, 197*, 331–337.

Sharififard, H. G., & mohaddeseh, Hosseinirad S,. (2018). Cadmium removal from wastewater using nano-clay/TiO_2 composite: Kinetics, equilibrium and thermodynamic study. *Advances in Environmental Technology, 4*, 203–209.

Sharifpour, E., Khafri, H. Z., Ghaedi, M., Asfaram, A., & Jannesar, R. (2018). Isotherms and kinetic study of ultrasound-assisted adsorption of malachite green and Pb^{2+} ions from aqueous samples by copper sulfide nanorods loaded on activated carbon: Experimental design optimization. *Ultrasonics Sonochemistry, 40*, 373–382.

Sharquie, K. E., Ibrahim, G. A., Noaimi, A. A., & Hamudy, H. K. (2011). Outbreak of thallium poisoning among Iraqi patients. *Journal of the Saudi Society of Dermatology & Dermatologic Surgery, 15*, 29–32.

Sheet, I., Kabbani, A., & Holail, H. (2014). Removal of heavy metals using nanostructured graphite oxide, silica nanoparticles and silica/graphite oxide composite. *Energy Procedia, 50*, 130–138.

Shirsath, D., Patil, B., & Shrivastava, D. (2013). Rapid removal of metals from aqueous solution by magnetic nanoadsorbent: A kinetic study. *International Journal of Nano Dimension*. 3, 303–312.

Shirsath, D., & Shirivastava, V. (2015). Adsorptive removal of heavy metals by magnetic nanoadsorbent: An equilibrium and thermodynamic study. *Applied Nanoscience, 5*, 927–935.

Singh, N., Rai, S., & Agarwal, S. (2014). Polymer nanocomposites and Cr (VI) removal from water. *Nanoscience and Technology, 1*, 1–10.

Sirviö, J. A., & Visanko, M. (2020). Lignin-rich sulfated wood nanofibers as high-performing adsorbents for the removal of lead and copper from water. *Journal of Hazardous Materials, 383*, 121174.

Soleimani, M., & Siahpoosh, Z. H. (2015). Ghezeljeh nanoclay as a new natural adsorbent for the removal of copper and mercury ions: Equilibrium, kinetics and thermodynamics studies. *Chinese Journal of Chemical Engineering, 23*, 1819–1833.

Šolić, M., Maletić, S., Isakovski, M. K., Nikić, J., Watson, M., Kónya, Z., & Rončević, S. (2021). Removing low levels of Cd (II) and Pb (II) by adsorption on two types of oxidized multiwalled carbon nanotubes. *Journal of Environmental Chemical Engineering, 9*, 105402.

Sun, Y., Zhou, S., Pan, S.-Y., Zhu, S., Yu, Y., & Zheng, H. (2020). Performance evaluation and optimization of flocculation process for removing heavy metal. *Chemical Engineering Journal, 385*, 123911.

Taffarel, S. R., & Rubio, J. (2010). Removal of Mn^{2+} from aqueous solution by manganese oxide coated zeolite. *Minerals Engineering, 23*, 1131–1138.

Taghavi, S. M., Momenpour, M., Azarian, M., Ahmadian, M., Souri, F., Taghavi, S. A., Sadeghain, M., & Karchani, M. (2013). Effects of nanoparticles on the environment and outdoor workplaces. *Electronic Physician, 5*, 706.

Takahashi, G. (2016). Damage and heavy metal pollution in China's farmland: Reality and solutions. *Journal of Contemporary East Asia Studies, 5*, 11–25.

Taman, R., Ossman, M., Mansour, M., & Farag, H. (2015). Metal oxide nano-particles as an adsorbent for removal of heavy metals. *Journal of Advanced Chemical Engineering, 5*, 1–8.

Team, & M. W. (2010). *Chemical precipitation*. Interstate Technology & Regulatory Council.

Tehrani, M. R. F., Shamsai, A., & Vossughi, M. (2015). In-situ Pb 2+ remediation using nano iron particles. *Journal of Environmental Health Science and Engineering, 13*, 1–8.

Thaçi, B. S., & Gashi, S. T. (2019). Reverse osmosis removal of heavy metals from wastewater effluents using biowaste materials pretreatment. *Polish Journal of Environmental Studies, 28*, 337–341.

Thakare, S., Mankar, M. A., & Puri, M. V. (2017). Removal of chromium from aqueous solution by using different methodologies. *International Research Journal of Engineering and Technology*. 4(5), 1408–1410.

Tiwari, A., Pal, D., & Sahu, O. (2017). Recovery of copper from synthetic solution by efficient technology: Membrane separation with response surface methodology. *Resource-Efficient Technologies, 3*, 37–45.

Tizro, S., & Baseri, H. (2016). Heavy metals removal from wastewater by using different kinds of magnetite nano-adsorbents: Effects of different organic and inorganic coatings on the removal of copper and lead ions. *Journal Advanced Materials and Processes, 4*, 15–29.

Tizro, S., & Baseri, H. (2017). Removal of cobalt ions from contaminated water using magnetite based nanocomposites: Effects of various parameters on the removal efficiency. *Journal of Water and Environmental Nanotechnology, 2*, 174–185.

Tran, H. N., You, S.-J., & Chao, H.-P. (2016). Thermodynamic parameters of cadmium adsorption onto orange peel calculated from various methods: A comparison study. *Journal of Environmental Chemical Engineering, 4*, 2671–2682.

Trinh, T. T. P. N. X., Quang, D. T., Tu, T. H., Dat, N. M., Linh, V. N. P., Loan, T. T., Hang, P. T., Phuong, N. T. L., Phong, M. T., & Nam, H. M. (2019). Fabrication, characterization, and adsorption capacity for cadmium ions of graphene aerogels. *Synthetic Metals, 247*, 116–123.

Tsuji, J. S., Maynard, A. D., Howard, P. C., James, J. T., Lam, C.-W., Warheit, D. B., & Santamaria, A. B. (2006). Research strategies for safety evaluation of nanomaterials, part IV: Risk assessment of nanoparticles. *Toxicological Sciences, 89*, 42–50.

Üzüm, Ç., Shahwan, T., Eroğlu, A. E., Lieberwirth, I., Scott, T. B., & Hallam, K. R. (2008). Application of zero-valent iron nanoparticles for the removal of aqueous Co^{2+} ions under various experimental conditions. *Chemical Engineering Journal, 144*, 213–220.

Valentín-Reyes, J., García-Reyes, R., García-González, A., Soto-Regalado, E., & Cerino-Córdova, F. (2019). Adsorption mechanisms of hexavalent chromium from aqueous solutions on modified activated carbons. *Journal of Environmental Management, 236*, 815–822.

Venkatesham, V., Madhu, G., Satyanarayana, S., & Preetham, H. (2013). Adsorption of lead on gel combustion derived nano ZnO. *Procedia Engineering, 51*, 308–313.

Venkateswarlu, S., Kumar, B. N., Prathima, B., SubbaRao, Y., & Jyothi, N. V. V. (2019). A novel green synthesis of Fe_3O_4 magnetic nanorods using *Punica Granatum* rind extract and its application for removal of Pb (II) from aqueous environment. *Arabian Journal of Chemistry, 12*, 588–596.

Venkateswarlu, S., Kumar, S. H., & Jyothi, N. (2015). Rapid removal of Ni (II) from aqueous solution using 3-Mercaptopropionic acid functionalized bio magnetite nanoparticles. *Water Resources and Industry, 12*, 1–7.

Vikrant, K., Kumar, V., Vellingiri, K., & Kim, K.-H. (2019). Nanomaterials for the abatement of cadmium (II) ions from water/wastewater. *Nano Research, 12*, 1489–1507.

Wang, H., Cui, H., Song, X., Xu, R., Wei, N., Tian, J., & Niu, H. (2020). Facile synthesis of heterojunction of MXenes/TiO_2 nanoparticles towards enhanced hexavalent chromium removal. *Journal of Colloid and Interface Science, 561*, 46–57.

Wang, J., Zheng, S., Shao, Y., Liu, J., Xu, Z., & Zhu, D. (2010). Amino-functionalized Fe_3O_4@ SiO_2 core–shell magnetic nanomaterial as a novel adsorbent for aqueous heavy metals removal. *Journal of Colloid and Interface Science, 349*, 293–299.

Wang, X., Guo, Y., Yang, L., Han, M., Zhao, J., & Cheng, X. (2012). Nanomaterials as sorbents to remove heavy metal ions in wastewater treatment. *Journal of Environmental & Analytical Toxicology, 2*, 154.

Wang, Z., Xu, J., Hu, Y., Zhao, H., Zhou, J., Liu, Y., Lou, Z., & Xu, X. (2016). Functional nanomaterials: Study on aqueous Hg (II) adsorption by magnetic Fe_3O_4@ SiO_2-SH nanoparticles. *Journal of the Taiwan Institute of Chemical Engineers, 60*, 394–402.

Wehbe, M., Tarboush, B. J. A., Shehadeh, M., & Ahmad, M. (2020). Molecular dynamics simulations of the removal of lead (II) from water using the UiO-66 metal-organic framework. *Chemical Engineering Science, 214*, 115396.

Wimalawansa, S. J. (2013). Purification of contaminated water with reverse osmosis: Effective solution of providing clean water for human needs in developing countries. *International Journal of Emerging Technology and Advanced Engineering, 3*, 75–89.

Xia, Z., Baird, L., Zimmerman, N., & Yeager, M. (2017). Heavy metal ion removal by thiol functionalized aluminum oxide hydroxide nanowhiskers. *Applied Surface Science, 416*, 565–573.

Yaghmaeian, K., Mashizi, R. K., Nasseri, S., Mahvi, A. H., Alimohammadi, M., & Nazmara, S. (2015). Removal of inorganic mercury from aquatic environments by multi-walled carbon nanotubes. *Journal of Environmental Health Science and Engineering, 13*, 1–9.

Yamini, Y., & Safari, M. (2018). Modified magnetic nanoparticles with catechol as a selective sorbent for magnetic solid phase extraction of ultra-trace amounts of heavy metals in water and fruit samples followed by flow injection ICP-OES. *Microchemical Journal, 143*, 503–511.

Yang, L., & Watts, D. J. (2005). Particle surface characteristics may play an important role in phytotoxicity of alumina nanoparticles. *Toxicology Letters, 158*, 122–132.

Yin, J., Deng, C., Yu, Z., Wang, X., & Xu, G. (2018). Effective removal of lead ions from aqueous solution using nano illite/smectite clay: Isotherm, kinetic, and thermodynamic modeling of adsorption. *Water, 10*, 210.

Yokoyama, H. (2018). *Lecture on methylmercury poisoning in minamata (MPM)*. Mercury Pollution in Minamata (pp. 5–51). Springer. 5–51.

Yoshida, F., Hata, A., & Tonegawa, H. (1999). Itai-Itai disease and the countermeasures against cadmium pollution by the Kamioka mine. *Environmental Economics and Policy Studies, 2*, 215–229.

You, H., Chen, J., Yang, C., & Xu, L. (2016). Selective removal of cationic dye from aqueous solution by low-cost adsorbent using phytic acid modified wheat straw. *Colloids and Surfaces a: Physicochemical and Engineering Aspects, 509*, 91–98.

Youzhi Li, Q. Z., Ren, B., Luo, J., Yuan, J., Ding, X., Bian, H., & Yao, X. (2020). Trends and Health Risks of Dissolved Heavy Metal Pollution in Global River and Lake Water from 1970 to 2017. *Reviews of Environmental Contamination and Toxicology, 251*, 1–24.

Yu, C., Shao, J., Sun, W., & Yu, X. (2020). Treatment of lead contaminated water using synthesized nano-iron supported with bentonite/graphene oxide. *Arabian Journal of Chemistry, 13*, 3474–3483.

Zandipak, R. (2017). Removal of Cr (VI) ions from aqueous solution usinf nickel ferrite nanoparticle: Kinetic and equilibrium study. *Arch Hyg Sci, 6*, 17–25.

Zare, E. N., Lakouraj, M. M., & Ramezani, A. (2016). Efficient sorption of Pb (II) from an aqueous solution using a poly (aniline-co-3-aminobenzoic acid)-based magnetic core–shell nanocomposite. *New Journal of Chemistry, 40*, 2521–2529.

Zarime, N. A., Yaacob, W. Z. W., & Jamil, H. (2018). Removal of heavy metals using bentonite supported nano-zero valent iron particles. In *AIP Conference Proceedings*, Vol. 1940. AIP Publishing LLC, p. 020029. 1940 (1).

Zawrah, M., & Alhogbi, B. G. (2021). Preparation and characterization of SiO_2@ C nanocomposites from rice husk for removal of heavy metals from aqueous solution. *Ceramics International, 47*, 23240–23248.

Zeinali, S., Abdollahi, M., & Sabbaghi, S. (2016). Carboxymethyl-β-cyclodextrin modified magnetic nanoparticles for effective removal of arsenic from drinking water: Synthesis and adsorption studies. *Journal of Water and Environmental Nanotechnology, 1*, 104–115.

Zewail, T., & Yousef, N. (2015). Kinetic study of heavy metal ions removal by ion exchange in batch conical air spouted bed. *Alexandria Engineering Journal, 54*, 83–90.

Zhan, W., Gao, L., Fu, X., Siyal, S. H., Sui, G., & Yang, X. (2019). Green synthesis of amino-functionalized carbon nanotube-graphene hybrid aerogels for high performance heavy metal ions removal. *Applied Surface Science, 467*, 1122–1133.

Zhang, F., Zhu, Z., Dong, Z., Cui, Z., Wang, H., Hu, W., Zhao, P., Wang, P., Wei, S., & Li, R. (2011). Magnetically recoverable facile nanomaterials: Synthesis, characterization and application in remediation of heavy metals. *Microchemical Journal, 98*, 328–333.

Zhou, C., Zhu, H., Wang, Q., Wang, J., Cheng, J., Guo, Y., Zhou, X., & Bai, R. (2017). Adsorption of mercury (II) with an Fe_3O_4 magnetic polypyrrole–graphene oxide nanocomposite. *RSC Advances, 7*, 18466–18479.